Newsletters on Stratigraphy
Published online March 2022

Prepub-Article
Open Access

A new age model and chemostratigraphic framework for the Maastrichtian type area (southeastern Netherlands, northeastern Belgium)

Johan Vellekoop[1,2]*, Pim Kaskes[1], Matthias Sinnesael[1,3], Jarno Huygh[1], Thomas Déhais[1], John W. M. Jagt[4], Robert P. Speijer[2] and Philippe Claeys[1]

With 6 figures and 1 table

Abstract. The youngest time interval of the Cretaceous Period is known as the Maastrichtian, in reference to the shallow-marine strata outcropping in the area surrounding the city of Maastricht, in the Netherlands-Belgium border region. While the type-Maastrichtian strata have yielded a wealth of paleontological data, comparatively little geochemical work has so far been carried out on this succession. To date, age assessment of the type-Maastrichtian, and stratigraphic correlation with sections elsewhere, have largely been based on biostratigraphy and preliminary attempts at cyclostratigraphy. However, these techniques are hampered by bio-provincialism and the presence of stratigraphic gaps in the succession, respectively. In recent years, stable carbon isotope stratigraphy has proven to be a powerful tool for correlating Upper Cretaceous strata on a global scale. When integrated with biostratigraphy, carbon isotope stratigraphy can be used to test the synchroneity of biological and climatic events across the globe and to reconcile inter-regional biostratigraphic schemes. Therefore, we have generated the first high-resolution bulk stable carbon isotope stratigraphy for the type-Maastrichtian, using an extensive sample set acquired within the context of the Maastrichtian Geoheritage Project spanning approximately 100 meters of stratigraphy at the Hallembaye and former ENCI quarries. In combination with bulk major and trace element data generated using μXRF, this record presents the first high-resolution chemostratigraphic survey for the type-Maastrichtian. The μXRF-based element profiles through the type-Maastrichtian succession reveal variable fluxes of terrigenous input into this carbonate system over time, marking three distinct stratigraphic sequences, separated by sequence boundaries at the Froidmont, Lichtenberg and Vroenhoven horizons. In addition, the carbon isotope profile records the Campanian–Maastrichtian Boundary Event (CMBE) and the Mid-Maastrichtian Event (MME) in the Maastrichtian type area for the first time. Our refined age model allows for global correlation between the type-Maastrichtian sequence and Maastrichtian successions worldwide and places the abundant paleontological records from the type-Maastrichtian in a global context.

Key words. Carbon-isotope stratigraphy, μXRF, chemostratigraphy, Maastrichtian type area

Authors' addresses:
[1] Analytical, Environmental and Geo-Chemistry Research Unit, Vrije Universiteit Brussel, Pleinlaan 2, B-1050 Brussels, Belgium; Pim.Kaskes@vub.be; jarno.huygh@hotmail.com; Thomas.Dehais@vub.be; phclaeys@vub.be
[2] Division Geology, KU Leuven, Celestijnenlaan 200E, 3001 Leuven, Belgium; johan.vellekoop@kuleuven.be; robert.speijer@kuleuven.be
[3] Department of Earth Sciences, Mountjoy Site, Durham University, South Road, DH1 3LE Durham, United Kingdom; matthias.sinnesael@durham.ac.uk
[4] Natuurhistorisch Museum Maastricht, de Bosquetplein 6-7, 6211 KJ Maastricht, the Netherlands; John.Jagt@maastricht.nl
* Corresponding author: johan.vellekoop@kuleuven.be

© 2022 The Authors
DOI: 10.1127/nos/2022/0703
Borntraeger Science Publishers, Stuttgart, www.borntraeger-cramer.com

1. Introduction

The youngest time interval of the Cretaceous Period is known as the Maastrichtian Stage, a reference to the marine strata exposed in the area surrounding the city of Maastricht, in the Netherlands-Belgium border region (Jagt 2001; Fig. 1). The stratigraphic succession at the original type-locality of the Maastrichtian (adjacent to the former ENCI quarry, south of Maastricht; Jagt 2001) only covers the upper part of the Maastrichtian Stage as defined nowadays (Odin and Lamaurelle 2001). However, in combination with similar lithological sequences that are accessible at other quarries in the region (e. g., Hallembaye, Curfs; Fig. 1), a substantial part of the Maastrichtian Stage is represented (Jagt and Jagt-Yazykova 2012). The highly fossiliferous sedimentary carbonate rocks in this region have generally been interpreted to have been deposited in a shallow, subtropical epeiric sea that flooded large parts of western Europe during the latest Cretaceous (Fig. 1; Jagt and Jagt-Yazykova 2012). Over the past centuries, the type-Maastrichtian strata have provided a wealth of paleontological data (e. g., Conybeare 1822, Leriche 1929, Dortangs et al. 2002, Madzia 2020, Field et al. 2020, Bastiaans et al. 2020, Vellekoop et al. 2020), comprising a wide array of vertebrate and invertebrate finds (Jagt 2015, Jagt et al. 2015; see Fig. 2). Numerous skeletal remains of e. g. mosasaurs, plesiosaurs, crocodiles, turtles and dinosaurs (Mulder et al. 1998), often disarticulated yet excellently preserved, have made the Maastrichtian type area a classic site in the history of paleontology (Dortangs et al. 2002). Nevertheless, so far, the age assessment of, and stratigraphic correlation with, the type-Maastrichtian strata has been largely based on lithostratigraphy (Felder 1975, Felder 2001), biostratigraphy (Schiøler et al. 1997, Jagt and Jagt-Yazykova 2012) and preliminary attempts at cyclostratigraphy (Zijlstra 1994, Keutgen 2018), techniques that are hampered by bio-provincialism (e. g. Robaszynski 1987, Christensen et al. 2000) and the presence of stratigraphic gaps in the succession (Vandenberghe et al. 2004, Keutgen and Jagt 2009), respectively. Up to now, comparatively little geochemical work has been carried out on this succession (e. g. Felder et al. 2003). As a result, the precise ages of some of the most crucial paleontological finds in the type-Maastrichtian, e. g., the recently discovered oldest known crown bird to date (Field et al. 2020), remain uncertain.

Stable carbon-isotope stratigraphy constitutes a powerful tool to better constrain the ages of the type-Maastrichtian strata, and thereby the paleontological records retrieved from these strata. In recent years, carbon-isotope stratigraphy has been highly effective to correlate Upper Cretaceous strata on a global scale, based on a succession of carbon isotope events in the geological record (Voigt et al. 2012, Thibault et al. 2012a, Wendler 2013, Eldrett et al. 2021). For the upper Campanian-Maastrichtian interval, Voigt et al. (2012) established a detailed carbon-

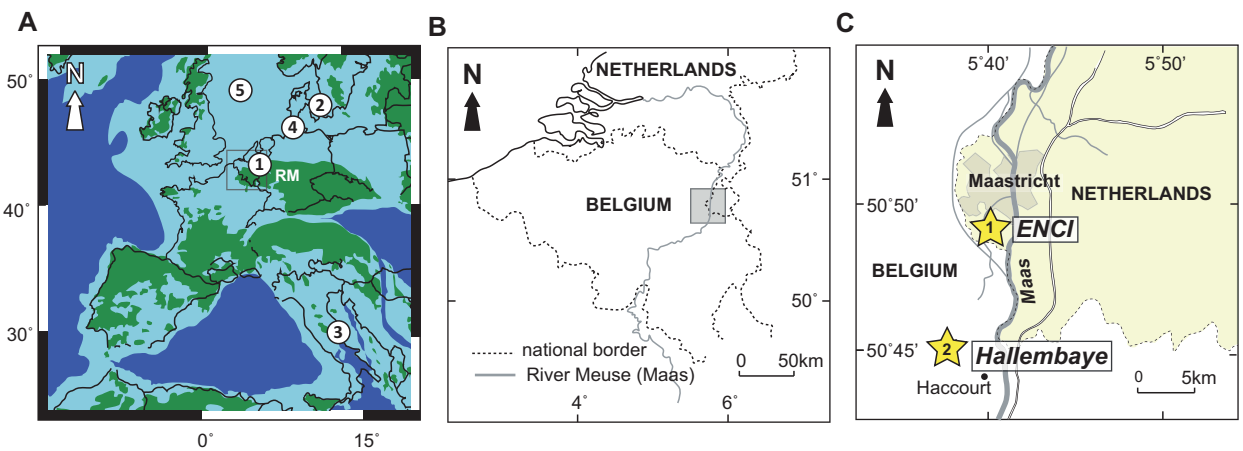

Fig. 1. **A.** Paleogeographic setting of western Europe during the Maastrichtian, after Vellekoop et al. (2019), with the Maastrichtian successions discussed in the text indicated. 1) Maastrichtian type area (Netherlands and Belgium); 2) Stevns-1 core (Denmark); 3) Gubbio composite (Italy), 4) Kronsmoor-Hemmoor (Germany); 5) Shearwater A9 well (central North Sea). RM = Rhenish Massif. Deep seas are shown in dark blue, shelf seas in light blue and landmasses in green. **B.** Geographic location of the Maastrichtian type area, in the Belgium-Netherlands border region. **C.** The Maastrichtian type area, with the locations of the former ENCI (1) and Hallembaye (2) quarries indicated.

isotope stratigraphy, recognizing a series of late Campanian (LCE), Campanian–Maastrichtian (CMBE-1 to CMBE-5), Mid-Maastrichtian (MME-1 to MME-3) and Cretaceous–Paleogene (KPgE-1 to KPgE-3) carbon-isotope events, which can be used to correlate Campanian–Maastrichtian record worldwide. Among the carbon-isotope events in the Maastrichtian age are three carbon-isotope shifts that together represent the elusive Mid-Maastrichtian Event (MME), an episode of widespread biotic and oceanographic changes, characterized by abrupt warming of surface and deep waters and the disappearance of the 'true' (i. e. non-tegulated) inoceramid bivalves (Frank et al. 2005, Dameron et al. 2017). The MME was presumably the result of a reorganization of oceanic circulation (Macleod 1994) and is possibly related to increased volcanic activity (Mateo et al. 2017). When calibrated with biostratigraphic events (Wendler 2013), carbon-isotope stratigraphy can be used to test the synchroneity of bio-events, reconcile inter-regional biostratigraphic schemes and provide improved age constrains on geochemical and paleontological data (Surlyk et al. 2013), placing the biotic records from the type-Maastrichtian in a global context. In addition, carbon-isotope stratigraphy presents a way to improve regional and global correlation with the type-Maastrichtian successions. Thibault et al. (2012a) published a very detailed, high-resolution, astronomically calibrated carbon-isotope stratigraphy for the Boreal Realm, which is particularly effective in correlating Campanian–Maastrichtian records from European sites (Fig. 1A), such as Stevns-1 (Denmark), Tercis-les-Bains (France), Gubbio (Italy), Norfolk (UK) and Kronsmoor and Hemmoor (Germany; Voigt et al. 2012). Correlation with the astronomically calibrated isotope record from Stevns-1 allows for an absolute age assessment of Maastrichtian strata throughout Europe.

Therefore, we have generated the first high-resolution (~30 cm) bulk carbonate stable carbon-isotope stratigraphy for the ~98 m thick composite succession of the type-Maastrichtian (Fig. 1B). For this, we employed the upper Campanian to lower/middle Maastrichtian Gulpen Formation strata exposed at the Hallembaye quarry (Haccourt, Belgium; Fig. 1C) and the strata of the middle to upper Maastrichtian Gulpen and Maastricht Formations exposed at the former ENCI quarry (Maastricht, the Netherlands; Fig. 1C), using an extensive sample set acquired within the context of the Maastrichtian Geoheritage Project (Vellekoop 2019). Over the past decades, extensive micro- and macropaleontological studies on these sites have resulted in a low-resolution nannofossil biostratigraphy (Čepek and Moorkens 1979, Robaszynski et al. 1985), in addition to well-constrained dinoflagellate cyst (Schiøler et al. 1997, Slimani 2000) and belemnite (Robaszynski 1985, Keutgen et al. 2010, Keutgen et al. 2019) biozonations for the type-Maastrichtian succession, which allow a calibration of the new stable carbon isotope record presented here. In addition, we have generated elemental data using micro-X-ray fluorescence (μXRF) analysis (e. g., Ca, Si, Al, Ti, Mn concentrations) on the same carbonate samples. Major and trace element compositions and ratios of carbonate rocks constitute powerful proxies for reconstructing regional paleoenvironmental, paleoceanographic and sequence stratigraphic changes, as illustrated by chemostratigraphic analysis of other Cretaceous carbonate successions (Jarvis et al. 2001). Our combined element and isotope record presents the first high-resolution chemostratigraphy for the type-Maastrichtian. This new chemostratigraphic framework refines the age-model and paleoenvironmental context for the studied strata and allows a better regional and global correlation with the type-Maastrichtian successions, placing the unique paleontological records from the type-Maastrichtian in a global context.

2. Geological setting

2.1. Hallembaye

The Hallembaye quarry (Belgium, 50°44'54" N, 5°38'54" E), formerly known as Ciment Portland Liégeois (CPL), currently Kreco, is situated on the left bank of the River Meuse (Maas), about 10 km south of Maastricht (Fig. 1). At present, approximately 50 meters of stratigraphy is exposed, consisting of flint-bearing calcilutites of the Gulpen Formation (Fig. 2). Given that the successions in the type-Maastrichtian consist of limestones that are mainly composed of detrital carbonate grains with a range of grain sizes, ranging from clay size to larger than sand size, we apply the limestone classification system of Grabau (1904), and use the term 'chalk' for calcilutites and calcilutites composed of calcareous nannofossil debris. The lithostratigraphy used here follows that of Felder (1975) and Felder and Bosch (2001). The base of the succession comprises ~12 meters of whitish, fine-grained chalk with rare black flint nodules (Zeven Wegen Member), capped by chalkstone and a prominent hardground, the

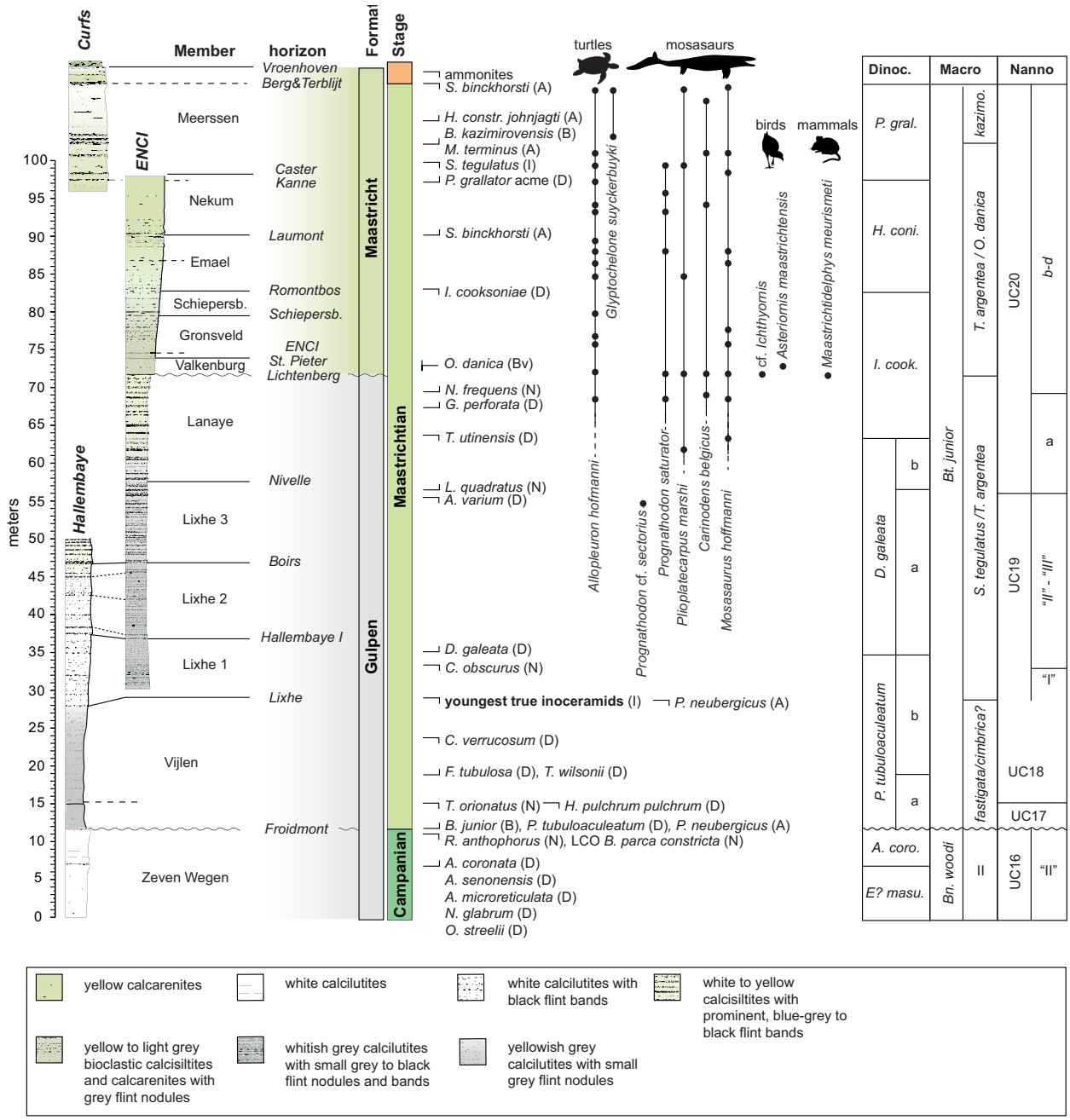

Fig. 2. Litho- and biostratigraphy of the type-Maastrichtian, with characteristic vertebrate finds. Dinocyst stratigraphy is based on Schiøler et al. (1997) and Slimani (2000), reconfigured by Keutgen (2018). Dashed lines indicate secondary lithological marker horizons. For completeness, the uppermost part of the succession, which was not targeted in this study, is also included in this figure, based on the stratigraphy of the former Curfs-Ankerpoort quarry (Vellekoop et al. 2020). Macrofossil stratigraphy is based on Voigt et al. (2008) and Jagt and Jagt-Yazykova (2018), nannofossil stratigraphy is based on Čepek and Moorkens (1979) and Robaszynski et al. (1985). Dinocyst (D), nannofossil (N), ammonite (A), belemnite (B), non-inoceramid bivalve (Bv) and inoceramid bivalve (I) bioevents are based on the above-mentioned publications, as well as on a compilation provided in Keutgen (2018). Characteristic turtle, mosasaur, bird, and mammal finds are based on Jagt and Jagt-Yazykova (2016) and Field et al. (2020) and references therein. Dinoc. = dinocysts, Macro. = macrofossil, Nanno = nannofossil stratigraphy. *E*? *masu* = *Exochosphaeridium*? *masureae*, *A. coro.* = *Areoligera coronata*, *I. cook.* = *Isabellidinium cooksoniae*, *H. coni.* = *Hystrichostrogylon coninckii*, *P. gral.* = *Palynodinium grallator.*

Froidmont Horizon. Overlying are ~16 meters of yellowish grey, fine-grained chalks with small grey flint nodules and bands (Vijlen Mb.). The basal part of this member is glauconite-rich. The Vijlen Mb. gradually passes into the white to yellowish white chalks with narrow, black-grey small flint bands of the Lixhe 1 Mb., which attains a thickness of ~9.5 meters. Above this are ~9.5 meters of white to yellowish white chalks with increasingly well-developed black flint bands (Lixhe 2 Mb.), overlain by ~3 meters of yellowish white chalks with thick, well-developed black flint bands (Lixhe 3 Mb.). The top 7 meters of the profile show discoloration indicative of weathering and leaching down from the overlaying soils.

Low-resolution nannofossil and belemnite biostratigraphy and detailed dinocyst biozonation document a middle to late Campanian age for the Zeven Wegen Member, while the Vijlen and Lixhe Members are Maastrichtian in age (Robaszynski et al. 1985, Keutgen and Jagt 1998, Slimani 2000). The Froidmont Hz. represents a stratigraphic hiatus of several million years, encompassing the Campanian–Maastrichtian boundary (Vandenberghe et al. 2004).

2.2. Former ENCI

The former ENCI quarry (the Netherlands, 50° 49'16"N, 5°41'15"E) is situated on the left bank of the River Meuse, approximately 2 km south of Maastricht (Fig. 1). The stratigraphic succession at this recently disused quarry comprises approximately 40 meters of flint-bearing calcilutites and calcisiltites of the Gulpen Formation and about 30 meters of bioclastic calcisiltites, calcarenites and calcirudites of the Maastricht Formation (Fig. 2). The current base of the succession consists of ~6.5 meters of whitish grey, fine-grained chalks with abundant small grey to black flint nodules and bands (Lixhe 1 Mb.), overlain by ~10 meters of fine-grained whitish grey chalk with increasingly well-developed black flint nodules and bands (Lixhe 2 Mb.), in turn followed by about 11 meters of whitish grey, fine-grained chalk with prominent black flint bands (Lixhe 3 Mb.). The top 14 meters of the Gulpen Fm. consist of increasingly silty, white to yellowish white chalks with abundant, very prominent, blue-grey to black flint bands and occasional small-scale trough cross bedding, fossil-rich lenses and discontinuous levels (Lanaye Mb.). The increasing grain size is the result of an increase in biogenic components, rather than a function of siliciclastic grains. The base of the overlying Maastricht Fm. consists of a lag deposit rich in fish coprolites, shark teeth and other macrofossils, the Lichtenberg Hz., followed by approximately 30 meters of highly fossiliferous, yellow to light grey, bioclastic calcisiltites, calcarenites and calcirudites of the Valkenburg, Gronsveld, Schiepersberg, Emael and Nekum Members of the Maastricht Fm., which are separated from each other by horizons with shell hash layers. The uppermost member of the Maastricht Fm., the Meerssen Mb., is also exposed at the former ENCI quarry, but could not be reached for sampling (Vellekoop 2019). The Maastricht Fm. shows a general increase in grainsize upwards, with predominantly calcisiltites and calcarenites in the Valkenburg and Gronsveld Members, calcarenites in the Schiepersberg, Emael and Nekum Members and calcarenites and calcirudites in the Meerssen Member. For a detailed description of the stratigraphic succession at the former ENCI quarry, see Felder and Bosch (1998).

Belemnite, nannofossil and dinocyst biostratigraphy document an early to late Maastrichtian age for the Gulpen Fm. at the former ENCI quarry, while the Maastricht Fm. is of late Maastrichtian age (Čepek and Moorkens 1979, Schiøler et al. 1997, Keutgen 2018). Low-resolution belemnite-based strontium isotope stratigraphy confirms this age assessment (Vonhof et al. 2011). According to the preliminary cyclostratigraphic age model proposed by Keutgen (2018), based on visual inspection of patterns in bioclasts rather than statistical analyses of high resolution lithological or geochemical data, the Lichtenberg Hz., separating the Gulpen and Maastricht Formations, represents a stratigraphic hiatus of approximately 700 kyrs.

3. Materials and Methods

3.1. Maastrichtian Geoheritage Project

The sample material used in this study was collected in 2018 and 2019 within the context of the Maastrichtian Geoheritage Project. The goal of this project is to preserve the geological heritage of the Maastrichtian type area by means of (1) digital imagery, using drone photogrammetry and differential GPS base & rover surveys (following Kaskes et al. 2017) in order to generate high-resolution and geo-referenced 3D-models of the most important quarries and outcrops in the Maastrichtian type region, and (2) archiving rock samples of these quarries for future research (Vellekoop 2019). For both the Hallembaye and former ENCI

quarries, which are c. 8 km apart, a 5 cm resolution sample set was acquired. A Jacob's staff with abney level and laser-pointer was used for accurate stratigraphic height measurements within and between subsections in the quarries. Outcrop surfaces were carefully cleaned and fresh, unweathered bulk (~25 cm^3) samples were collected at a 5 cm stratigraphic resolution. All samples obtained within the context of the Maastrichtian Geoheritage Project are stored at the Natural History Museum of Maastricht (NHMM). The combined succession of close to 98 meters of stratigraphy comprises ~72 m of the upper Campanian and lower Maastrichtian Gulpen Formation and ~26 meters of the upper Maastrichtian Maastricht Formation (Fig. 2). There is ~15 m of stratigraphic overlap between the successions exposed at Hallembaye, and that exposed at the former ENCI. Correlation between these quarries was done using the characteristic Boirs Hz., a marker that can be traced throughout the region (Felder and Bosch 2000), to arrive at a composite height for the record, in meters composite height (mch). A subset of the 5 cm resolution sample set of the Maastrichtian Geoheritage Project was used in the present study, after the samples were dried for 1 week at 40 °C and subsequently carefully ground to homogeneous powders using mortar and pestle.

3.2. µXRF

The major and trace element composition of bulk carbonate samples was measured on a total of 146 samples from Hallembaye and 184 samples from the former ENCI, resulting in a mean sampling resolution of c. 35 cm for each site (Supplementary Table 1). The element composition was determined by means of micro-X-ray fluorescence (µXRF) analysis at the laboratory of the Analytical, Environmental and Geo-Chemistry Research Unit (AMGC) of the Vrije Universiteit Brussel (Brussels, Belgium; VUB). This novel geochemical technique allows rapid, non-destructive and high-resolution analysis of flat sample surfaces for semi-quantitative element mapping, as well as quantitative linescans and spot analysis with a resolution down to 25 µm (de Winter and Claeys 2017; Kaskes et al. 2021). Both portable and laboratory benchtop XRF analyses have shown to provide reliable and reproducible major and trace element compositions for carbonate materials (de Winter et al. 2017), thereby offering valuable insights into paleoenvironmental changes across stratigraphic intervals (Sinnesael et al. 2018). For the present study, repeated spot analysis on homogeneous carbonate powders was carried out using an M4 Tornado benchtop µXRF instrument (Bruker nano GmbH, Berlin, Germany) equipped with a 30 W Rh tube as X-ray source, a polycapillary X-ray lens and two XFlash 430 Silicon Drift detectors. After the powders were carefully flattened and mounted in a holder with plastic cups, spot analysis was performed using both detectors at maximized X-ray source energy settings (50 kV and 600 µA, without an X-ray source filter). The measurements were carried out under near-vacuum conditions (20 mbar) using 10 points per powder and an integration time of 120 s for a spotsize of 25 µm. This integration time was selected to allow the Time of Stable Reproducibility and Time of Stable Accuracy to be reached, which allows the concentration of a range of elements to be quantified (de Winter et al. 2017). The resulting XRF spectra were quantified using a matrix corrected Fundamental Parameters method (de Winter and Claeys 2017) and then calibrated following the procedures outlined in De Winter et al. (2021). This multi-standard calibration used repeated µXRF spot-analysis on a set of 10 carbonate certified reference materials: CRM393 (Bureau of Analyzed Samples Ltd, Middlesbrough, UK; BAS), CRM512 (BAS), CRM513 (BAS), ECRM782 (BAS), CCH1 (Université de Liège, Belgium), COQ1 (United States Geological Survey, Denver, CO, USA), SRM1d (National Institute of Standards and Technology, Gaithersburg, MD, USA), NIM-GBW07108 (China National Analysis Center for Iron and Steel, Beijing, China; NCS), NIM-GBW07714 (NCS) and NIM-GBW07717 (NCS). Repeated µXRF spotanalysis of the above-mentioned carbonate standards resulted in a reproducibility for all reported major and trace elements (Al, Si, Ca, Ti, Mn) of <15 % relative standard deviation (de Winter and Claeys 2017). The resulting concentrations for the 10 individual points per powdered sample were processed by flagging and removing any outliers using the robust median absolute deviation as an estimator for scale (Rousseeuw and Croux 1993, Leys et al. 2013) before calculating the average concentration per element. Per sample, the data was expressed as element ratios and as normalized, volatile-free bulk oxide or carbonate values in wt%, to be able to display for instance bulk $CaCO_3$ variations versus stratigraphic height.

3.3. Isotope ratio mass spectrometry

The stable oxygen and carbon isotopic composition of bulk carbonates was measured on a total of 110 samples from Hallembaye and 250 samples from

the former ENCI, resulting in a mean sampling resolution of c. 30 cm for each site (**Supplementary Table** 2). Stable isotope ratio measurements were performed at the AMGC laboratory of the VUB (Belgium). Aliquots of ±50 μg of homogeneous carbonate powder were allowed to react with 104 % phosphoric acid (H_3PO_4) at 70 °C in a Nu-Carb carbonate preparation device and stable oxygen and carbon isotope ratios ($\delta^{18}O$ and $\delta^{13}C$) were measured using a Nu Perspective isotope ratio mass spectrometer (Nu Instruments Ltd, Wrexham, UK). All isotope ratio values are reported in ‰, relative to the Vienna Pee Dee Belemnite standard (‰ VPDB). Calibration to the V-PDB standard via NBS-19 was made using the AMGC in-house Marbella limestone standard (MAR 2-2, +3.41‰ VPDB $\delta^{13}C$, –0.13‰ VPDB $\delta^{18}O$). About 10 % of samples were run in duplicate. The reproducibility of repeated measurements was better than 0.1‰ (one standard deviation) for both oxygen and carbon isotope ratios.

4. Results

4.1. Major and trace element composition

The lowermost member of the studied succession, the upper Campanian Zeven Wegen Mb., is comprised of monotonous, relative pure, whitish chalks, with bulk $CaCO_3$ contents up to 97 wt% (Fig. 3). This member is capped by the Froidmont Hz. (11.75 mch), which marks a sharp transition in the record, to the considerably less pure, yellowish grey, fine-grained chalks of the Vijlen Mb. The lower 4 meters of that unit generally comprise less than 85 wt% $CaCO_3$, with a minimum of 68 wt% $CaCO_3$ at the base of the member. The transition across the Froidmont Hz. (11.75 mch) is also clear, with a major elevation in the Si/Ca, Al/Ca, and Ti/Ca records, suggesting a dilution of carbonates by terrigenous material. In the upper 12 meters of the Vijlen Mb. the $CaCO_3$ content gradually increases to up to 94 wt%, paralleled by decreasing Si/Ca, Al/Ca, and Ti/Ca values. This trend of increasing carbonate content continues in the overlying members of the Gulpen Formation, to reach 95–96 wt% $CaCO_3$ in the uppermost member of that formation, the Lanaye Member. At the former ENCI quarry, the Lixhe Members are characterized by a slightly lower $CaCO_3$ content (68–94 wt%), compared to their equivalent at the Hallembaye quarry (92–98 wt%). The base of the Maastricht Fm. (71.70 mch) is characterized by a drop in $CaCO_3$ content, to values around 87–93 wt%, accompanied by a sharp increase in Si/Ca, Al/Ca and Ti/Ca values, indicating a relatively higher terrigenous input. The overlying Gronsveld Mb. is characterized by a further decrease in $CaCO_3$ content, reaching a minimum of 45 wt% close to the ENCI Hz. (74.7 mch). This interval shows the highest Si/Ca, Al/Ca, and Ti/Ca values of the investigated succession. The basal interval of the Maastricht Fm. clearly received a relatively high influx of terrigenous material. Through the remainder of the Gronsveld Mb., $CaCO_3$ content steadily increases again, reaching values close to 95 % in the upper part of this member. The overlaying Schiepersberg Mb. shows another drop in $CaCO_3$ content, reaching a minimum of 80 wt%. The succeeding Emael Mb. is characterized by varying $CaCO_3$ content, ranging from 87 to 96 wt%, whereas the overlying Nekum Mb. comprises relatively pure calcarenites, with approximately 97 wt% $CaCO_3$. The succession is characterized by high values of Mn/Al (0.02–0.2) compared to the European average shale (0.01; Wedepohl 1971). In general, the variations in Mn/Al follow those in the bulk $CaCO_3$ contents, with increasing values towards the Froidmont and Lichtenberg horizons and a drop across these horizons.

4.2. Stable isotopes

Carbon isotope values range between 1.27‰ and 1.95‰ in the Hallembaye record and between 1.30‰ and 2.05‰ in the ENCI record (Fig. 3). Oxygen isotope values range between –1.76‰ and –0.93‰ in the Hallembaye record and between –3.09‰ and –0.01‰ in the ENCI record (Fig. 4). Since the top 7 meters of the profile of Hallembaye show signs of severe weathering and leaching down from the overlaying soils, samples from this interval were not included in the stable isotope analyses. A crossplot of carbon and oxygen isotopes is commonly used to test a possible diagenetic overprint which would result in a positive correlation between the two ratios (Jenkyns et al. 1995; Mitchell et al. 1997). In the stable isotope record of the dataset of the Maastrichtian type area, a crossplot shows no linear correlation of $\delta^{18}O$ and $\delta^{13}C$ values ($R^2 = 0.04$, p-value < 0.01; Fig. 4), suggesting an overall low diagenetic overprint (Thibault et al. 2012b). Nevertheless, a subset of samples from the lower 25 meters of the Gulpen Fm. of the former ENCI quarry does show a positive correlation between $\delta^{18}O$ and $\delta^{13}C$ ($R^2 = 0.5$, p-value < 0.01). Fortunately, the lower ratio of carbon in interstitial fluids with respect to carbon in carbonate as compared

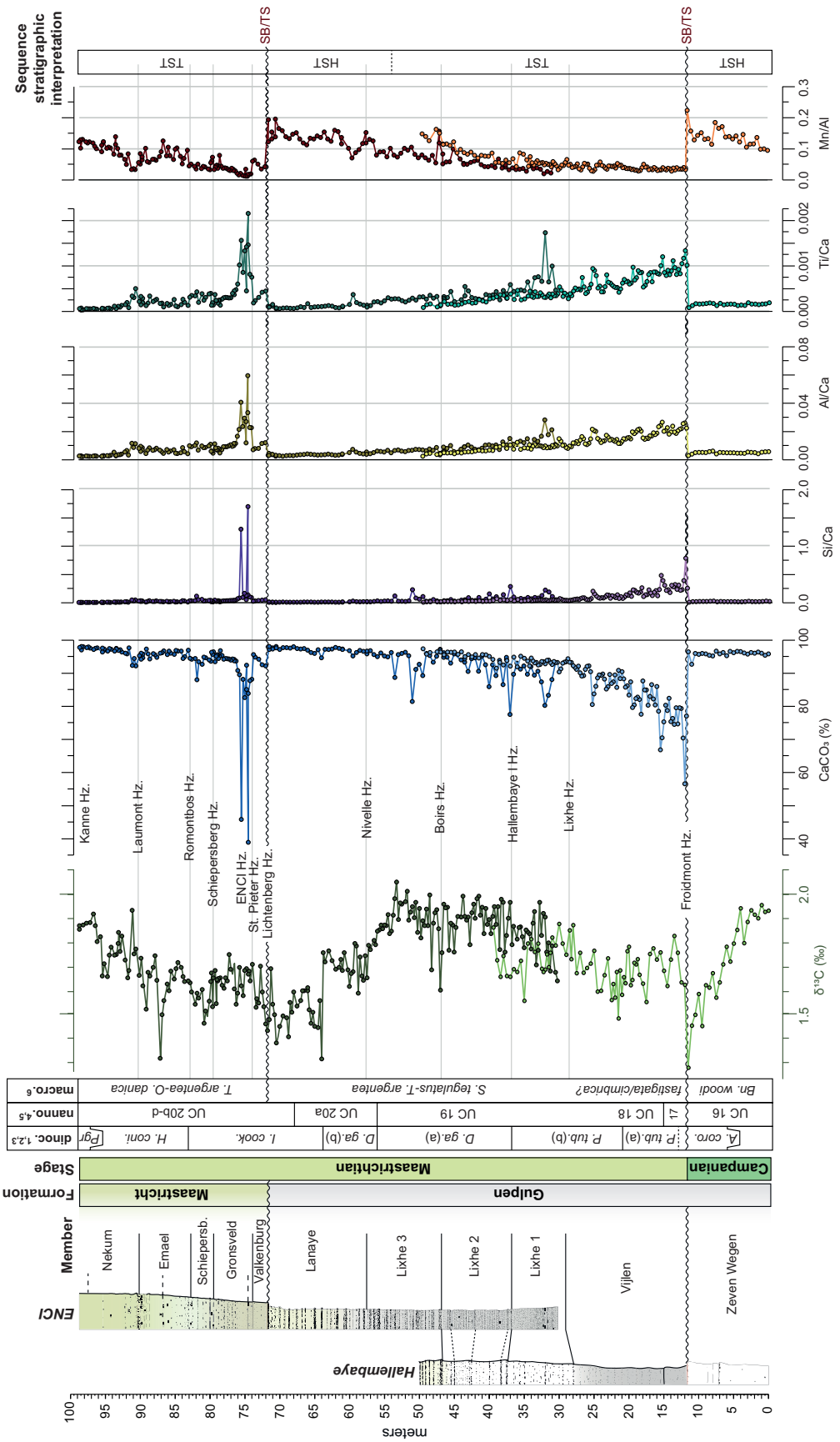

Fig. 3. Bulk stable carbon isotope ratio profiles (‰ VPDB) of the Hallembaye and former ENCI quarries and bulk $CaCO_3$ content and Si/Ca, Al/Ca, Ti/Ca and Mn/Al element ratios, based on µXRF analyses. References: 1) Schiøler et al. (1997); 2) Slimani (2000); 3) Keutgen (2018); 4) Čepek and Moorkens (1979); 5) Robaszynski et al. (1985); 6) Voigt et al. (2008). Sequence stratigraphic interpretation is based on µXRF-based element profiles and sedimentology. HST = Highstand Systems Tract, TST = Transgressive Systems Tract, SB = Sequence Boundary, TS = Transgressive Surface.

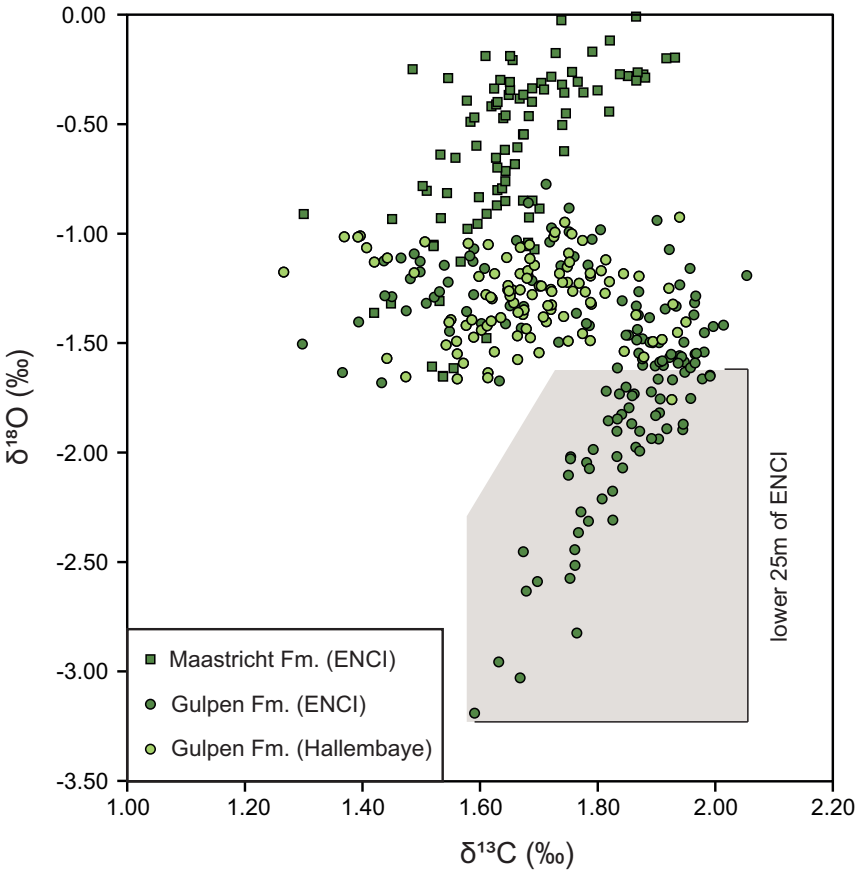

Fig. 4. A cross-plot of bulk carbon- and oxygen-isotope ratios (‰ VPDB) analyzed from the Maastrichtian type area (Hallembaye and former ENCI quarries). Taken together, the entire dataset shows no correlation of $\delta^{18}O$ and $\delta^{13}C$ values ($R^2 = 0.04$, p-value < 0.01). However, a subset of samples from the lower 25 meters of the Gulpen Fm. of the former ENCI quarry does show a positive correlation between $\delta^{18}O$ and $\delta^{13}C$ ($R^2 = 0.5$, p-value < 0.01), suggesting a possible diagenetic overprint for this part of the succession.

to the similar ratio of oxygen (Schrag et al. 1995) means that the bulk carbon isotopic signal is less sensitive to diagenetic alteration than oxygen isotopes. Therefore, while the observed correlation in the lower part of the Gulpen Fm. of the former ENCI quarry could have been partially driven by diagenetic overprint of $\delta^{18}O$, the $\delta^{13}C$ is considered to represent a primary signal. The bulk stable oxygen isotope profile of the type-Maastrichtian shows a distinctive pattern, with lower (–3.00 to –1.50 ‰) and intermediate (–1.50 to –1.00 ‰) values throughout the Gulpen Fm., and a general increasing trend (–1.75 to 0.00 ‰) throughout the Maastricht Fm. (Fig. 4). While these trends might point towards variations in diagenetic overprint, they could also be influenced by long term trends in environmental conditions through the succession.

The stable carbon isotope profile of the studied succession exhibits several positive and negative excursions and inflection points (Fig. 3). The basal part of the upper Campanian Zeven Wegen Member shows a plateau at ~1.95‰, followed by a decreasing trend, reaching ~1.25‰ at the Froidmont Horizon. The stratigraphic hiatus across this horizon is marked by ~0.5 permille jump, to lowermost Maastrichtian values of ~1.70‰. The lower Maastrichtian Vijlen Member is characterized by fluctuating values, followed by a stepwise decrease, reaching a minimum of 1.50‰ in the upper part of the member (at 24–25 m in the Hallembaye record). From the upper part of the Vijlen Mb. to the base of the Lixhe 2 Mb., a stepwise increasing trend occurs, of about 0.25‰, followed by stable values around 1.95‰ up to the middle of the Lixhe 3 Mb., where the record reaches maximum values of ~2.00‰. This plateau, from the base of the Lixhe 2 Mb. to the middle of the Lixhe 3 Mb., is superimposed by several, short, ~0.2–0.3 permille negative excursions, predominantly at the top of the Lixhe 2 Mb. (Fig. 3). After the maximum in the middle of the Lixhe 3 Mb., the remainder of the Gulpen Fm. is characterized by a stepwise decreasing trend, reaching values of ~1.40‰ near the top of the Lanaye Mb. The middle of that unit is characterized by an abrupt negative 0.3 permille excursion, above flint marker bed L10 (Felder and Bosch 1998). The lowermost

2.5 meters of the overlying Maastricht Fm. (representing the Valkenburg Mb.) again shows ~0.2–0.3 permille high frequency variability. The basal part of the Gronsveld Mbr is characterized by average values of ~1.70‰, above which the values gradually decrease, reaching a minimum of ~1.45‰ in the Schiepersberg Member. Above, there is an irregular increasing trend, interrupted by several spikes consisting of one or two data points. Maximum values of ~1.90‰ are reached in the basal part of the Nekum Member. In the top part of the profile, within the Nekum Mb values fluctuate around the maximum of 1.70–1.95‰.

5. Discussion

5.1. Terrigenous input and sequence stratigraphy

The predominant carbonate sedimentation in the type-Maastrichtian during the Campanian–Maastrichtian suggests a relatively large distance to emergent hinterlands, such as the Rhenish Massif and adjacent Bohemian Massif to the southeast (Fig. 1A). This is corroborated by the generally very low input of terrestrial palynomorphs (sporomorphs) throughout most of the studied succession (Schiøler et al. 1997). Nevertheless, several levels within the Maastricht Fm. are known for occasional finds of terrestrial fossils (Fig. 2), such as sporadic driftwood (Jagt and Collins 1999, Donovan and Jagt 2013), conifer foliage and seed cones (Van der Ham and Van Konijnenburg-van Cittert 2003, Van der Ham et al. 2003, Ham et al. 2010) and rare vertebrate remains, including both avian and non-avian dinosaurs and rare mammals (Jagt et al. 2003, Martin et al. 2005, Field et al. 2020). The majority of these remains are considered to have been washed into the sea by rivers and transported over considerable distances, as driftwood and floating corpses, respectively (e. g., Jagt and Collins 1999). Within the Maastricht Fm., terrestrial material seems to be most prevalent in the basal part of the Gronsveld Mb. and to a lesser extent in the Valkenburg and Emael Members, as well as at the base of the Nekum Mb. (Jagt and Collins 1999, Van der Ham and Van Konijnenburg-van Cittert 2003, Van der Ham 2003, Jagt et al. 2003).

The μXRF-based element profiles of our 98 m thick studied stratigraphic succession provide new insights into the variations in terrestrial input during the deposition of large parts of the Gulpen and Maastricht Formations of the type-Maastrichtian area (Fig. 3). The succession is characterized by biogenically produced carbonates ($CaCO_3$) with various degrees of dilution by terrigenous material, represented by increased concentrations of predominantly terrestrial-derived elements such as Al and Ti. These elements are likely largely present in the form of clay minerals (Wedepohl 1971), that were most probably transported into the carbonate system by either riverine or aeolian processes. The type-Maastrichtian record shows a distinctive pattern, with repeated successions of progressively more pure carbonates, capped by unconformities. The lowermost studied interval (c. 12 m thick), i. e. the topmost part of the upper Campanian Zeven Wegen Mb. represents the final stage of such a succession, an interval with very low terrigenous input (<5 %) capped by the Froidmont Hz. unconformity. The overlying interval (c. 61 m thick) of the Vijlen, Lixhe 1 to 3 and Lanaye Members represents a second succession, with relatively high terrigenous input (20–25 %) at its base, overlain by increasingly pure carbonates, reaching values similar to those of the Zeven Wegen Mb. in the upper half of the Lanaye Mb. (~5 % terrigenous material). This succession is capped by the Lichtenberg Hz. unconformity. The basal part (~25 m) of the overlying Maastricht Fm. is again characterized by relatively high terrigenous input, reaching its highest values (~50 %) in two levels in the basal part of the Gronsveld Mb., corresponding to a heavily burrowed interval rich in clay lenses and clay rip-up clasts, in between the St. Pieter and ENCI horizons. The clay lenses and rip-up clasts in this interval are clear indicators of transport of terrigenous clays into the carbonate environment. A second peak of terrigenous material (~20 %) occurs near the top of the Schiepersberg Mb. This lower part of the Maastricht Fm. shows the highest input of terrigenous material of the entire studied succession, which is consistent with the prevalent terrestrial macrofossils in this stratigraphic interval. Above the Schiepersberg Mb., the remainder of the Maastricht Fm. is again characterized by increasingly pure carbonates upwards, reaching values similar to the Zeven Wegen Mb. in the upper half of the Nekum Mb. (<5 % terrigenous material). The Meerssen Mb., which rests on top of the Nekum Mb., was not included in the present study, but previous work has shown that this member is also characterized by very pure carbonates (Felder and Bosch 2000) and is capped by the Vroenhoven Hz., which represents another stratigraphic hiatus (Vellekoop et al. 2020).

This pattern of repeated successions of progressively more pure carbonates capped by stratigraphic unconformities, strongly suggests a sequence stratigraphic control on this marine depositional system (Van Wagoner et al. 1988). If correctly interpreted, the Froidmont, Lichtenberg and Vroenhoven horizons each represent sequence boundaries, while the correlative hiatuses would likely reflect non-deposition or erosion during regressive and lowstand phases (Vandenberghe et al. 2004), expressed as hardgrounds and omission surfaces in the stratigraphic record (Fig. 3). During the transgressive phases (Transgressive Systems Tract, TST), deposition of increasingly pure carbonates occurred, as the distance to emergent hinterlands progressively became greater. Near the top of the sequences, represented by the Lanaye and Meerssen Members, respectively, increasing grain-size suggests increasingly stronger hydrodynamic conditions. This might have been caused by falling relative sea level, as sediment accumulation rates exceeded the rate of relative sea level rise (Highstand Systems Tract, HST; Fig. 3). Both the Lanaye and Meerssen Members are subsequently capped by a sequence boundary, i. e. the base of a new sequence. This sequence stratigraphic pattern can also be deduced from Mn/Al ratios throughout the record (Fig. 3). Manganese content is a useful proxy in sequence stratigraphy, as it has been shown that the Mn flux in pelagic and hemipelagic carbonate sedimentary systems increases during transgressive phases (Jarvis et al. 2001). Lowstand system tracts have usually low Mn and low Mn/Al contents, transgressive systems tracts display rising Mn/Al values with maxima around maximum flooding surfaces (Olde et al. 2015). The correlation between Mn/Al and sea level might be related to increased productivity during sea-level rise, promoting increased organic matter-associated particulate Mn flux to the sea floor (Jarvis et al. 2001). The highest Mn/Al values in the studied succession have been found just below the hardground/omission levels of the Froidmont and Lichtenberg horizons, which is consistent with data from hardgrounds in Cretaceous chalk sequences of northern France, the southern UK and southern Belgium (Jarvis 1992). These hardgrounds are characterized by sediment omission and/or erosion and the high Mn contents might be linked to lower sedimentation rates that led to increased efficiency of the Mn redox cycling (Jarvis et al. 2001). The relatively high values of Mn/Al (0.02–0.2) compared to the European average shale (0.01; Wedepohl 1971) indicate well-oxygenated bottom waters throughout the succession (Niebuhr 2005).

5.2. Correlation with other Upper Cretaceous records

Bulk carbon isotope records represent a robust stratigraphic tool for regional and sub-regional correlation of Upper Cretaceous successions (Voigt et al. 2012, Thibault et al. 2012a, Wendler 2013, Eldrett et al. 2021). Given that the chalks of the Gulpen Fm. are mainly composed of calcareous nannofossil debris, $\delta^{13}C$ values likely reflect primary sea-surface water values with any diagenetic effects affecting the formation in a consistent manner. In contrast, the bioclastic calcisiltites and calcarenites of the Maastricht Fm. predominantly consist of debris of macrobenthic organisms such as bryozoans, echinoderms and mollusks (Felder 2001). As different calcifiers (coccoliths vs. different groups of macro-organisms) are likely influenced by different vital effects, this formation might show a different carbon isotope signature. Moreover, the $\delta^{13}C$ values of these benthic organisms will reflect bottom-water instead of pelagic values. Nonetheless, as the Maastricht Fm. was deposited in a hydrodynamically high-energy setting at shallow depositional depths (~20–40 m, Voigt et al. 2008), the water column was likely well mixed during the deposition of this formation, resulting in little difference between sea-surface and bottom-water $\delta^{13}C$ values. Therefore, the stable carbon-isotope profile of the entire succession likely reflects primary upper water column values. Hence, the positive and negative excursions and inflection points in the carbon-isotope profiles of the type-Maastrichtian can be used for a regional correlation (Fig. 5). Our stable carbon isotope record shows a particularly strong resemblance to the astronomically calibrated isotope records from Gubbio (Italy, Voigt et al. 2012; Batenburg et al. 2018 and other records in Europe, such as Stevns-1 in Denmark (Thibault et al. 2012a), Kronsmoor/Hemmoor, (Germany, Voigt et al. 2010),) and the Shearwater A9 well (central North Sea; Eldrett et al. 2021), allowing for regional and global correlations (Fig. 5).

The carbon isotope profile of the upper Campanian Zeven Wegen Mb. shows a plateau phase, followed by a ~0.75‰ decrease. This interval correlates with nannofossil zone UC16 (Robaszynski et al. 1985) and the *Areoligera coronata* dinocyst Zone (Slimani 2000), indicating that it corresponds to the CMBE-1 and CMBE-2 carbon isotope events of Voigt et al. (2012), respectively. Carbon isotope event CMBE-2 of Voigt et al. (2012) equates with carbon isotope event CMB-a of Thibault et al. (2012a). The Highest Occur-

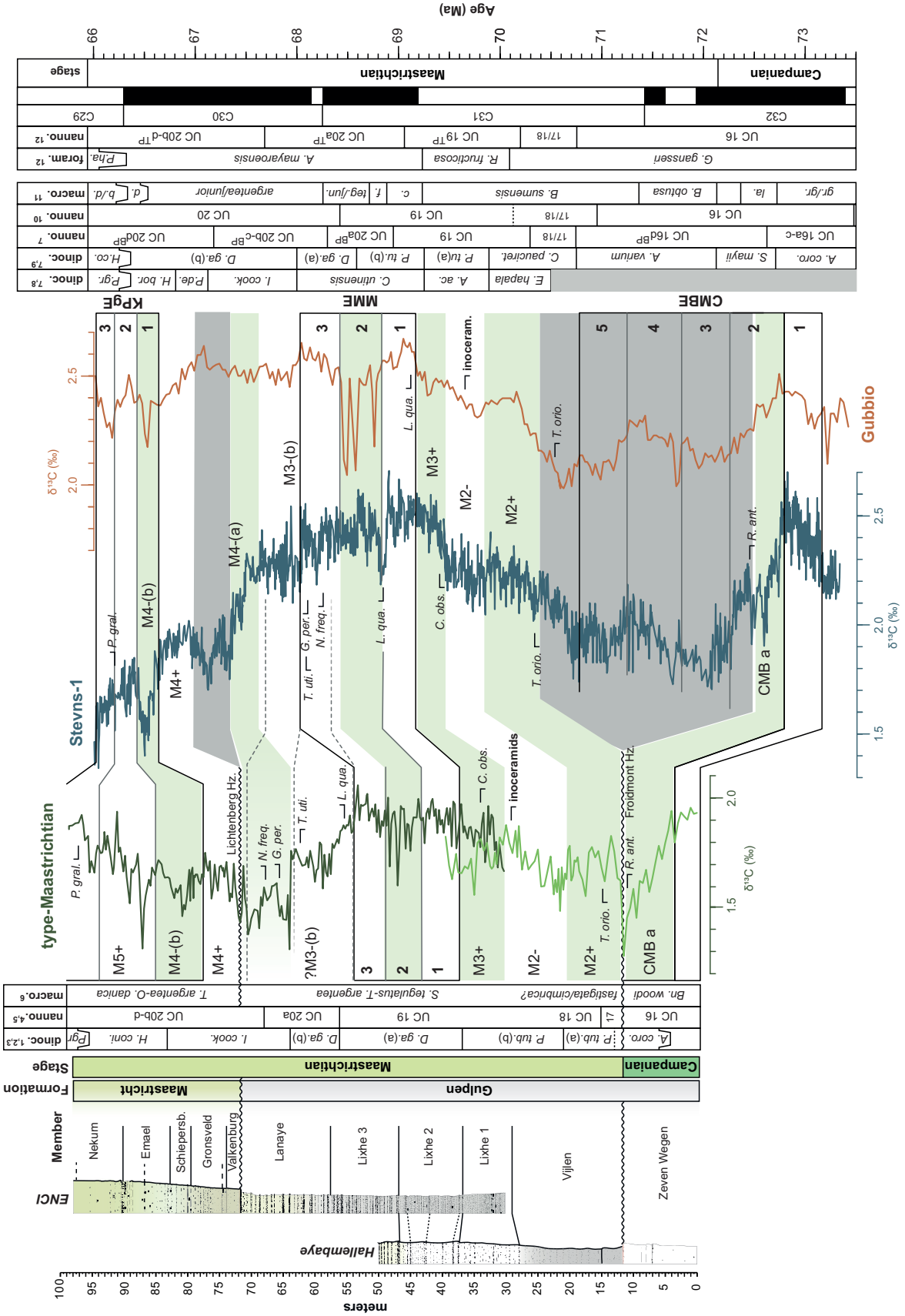
Age (Ma)
stage
Campanian
Maastrichtian
nanno.12
UC 16
UC 19TP
UC 20aTP
UC 20b-dTP
C32
C31
C30
C29
foram.12
G. gansseri
R. fructicosa
A. mayaroensis
P.Pla.
dinoc.7,8
E. hapala
A. ac.
C. utinensis
I. cook.
P.de.
H. bor.
P.gr.
C. pauciret.
P. tu(a)
P. tu.(b)
D. ga.(a)
D. ga.(b)
H.co.
A. coro.
S. mayii
A. varium
P. tub.(a)
P. tub.(b)
D. ga.(a)
D. ga.(b)
I. cook.
H. coni.
Pgr.
nanno.7
UC 16a-c
UC 16dBP
17/18
UC 19
UC 20aBP
UC 20b-cBP
UC 20d BP
nanno.10
UC 16
17/18
UC 19
UC 20
macro.11
gr./gr.
Ia.
B. obtusa
B. sumensis
c.
f.
tag./jun.
argentea/juvenior
d.
b./d.
KPgE
MME
CMBE
Stevns-1
Gubbio
type-Maastrichtian
δ13C (‰)
meters
Member
Formation
Stage
ENCI
Hallembaye
Nekum
Emael
Schiepersb.
Gronsveld
Valkenburg
Lanaye
Lixhe 3
Lixhe 2
Lixhe 1
Vijlen
Zeven Wegen
Maastricht
Gulpen
Campanian
Maastrichtian
dinoc.1,2,3
nanno.4,5
macro.6
A. coro.
P. tub.(a)
P. tub.(b)
D. ga.(a)
D. ga.(b)
I. cook.
H. coni.
UC 16
UC 18
UC 19
UC 20a
UC 20b-d
Bn. woodi
fastigata/cimbrica?
S. tegulatus-T. argentea
T. argentea-O. danica
M5+
M4-(b)
M4+
?M3-(b)
M3+
M2-
M2+
CMB a
M4-(a)
M3-(b)
P. gral.
Lichtenberg Hz.
N. freq.
G. per.
T. uti.
L. qua.
C. obs.
inoceramids
T. orio.
R. ant.
Froidmont Hz.
inoceram.

Fig. 5. Correlation of the new upper Campanian–Maastrichtian $\delta^{13}C$ record of the type-Maastrichtian to the Stevns-1 and Gubbio records, showing carbon isotope events CMB-a to M5+ of Thibault et al. (2012a), including the Campanian–Maastrichtian Boundary Event (CMBE), Mid-Maastrichtian Event (MME) and Cretaceous–Paleogene Event (KPgE). Bulk carbonate $\delta^{13}C$ data from Stevns-1 (Denmark) are from Thibault et al. (2012a), and those for Gubbio (Italy) are from Voigt et al. (2012). The Gubbio record is recalibrated by Batenburg et al. (2018). For the upper Lixhe 3 and Lanaye, two options are considered: option 1, primarily based on the isotope stratigraphy, is indicate by the green bars, option 2, based on the biostratigraphy and isotope stratigraphy, is indicated by dashed lines. For the biostratigraphy of the type-Maastrichtian, see Fig. 2. Biostratigraphic markers used as tie-points are indicated in the figure. The age model is based on the ages of geomagnetic reversals as indicated in Gale et al. (2020). References: 1) Schiøler et al. (1997); 2) Slimani (2000); 3) Keutgen (2018); 4) Čepek and Moorkens (1979); 5) Robaszynski et al. (1985); 6) Voigt et al. (2008); 7) Surlyk et al. (2013); 8) Schiøler and Wilson (1993); 9) Slimani et al. (2011); 10) Burnett (1990); 11) Schulz et al. (1984); 12) Gardin et al. (2012). *R. ant. = Reinhardtites anthophorus*, *T. orio. = Tranolithus orionatus*, *C. obs. = Calculites obscurus*, *L. qua. = Lithraphidites quadratus*, *T. uti. = Triblastula utinensis*, *G. per. = Glaphyrocysta perforata*, *N. freq. = Nephrolithus frequens*, *P. gral. = Palynodinium grallator*, *inoceram. = non-tegulated inoceramids*, *A. ac. = Alterbidinium acutulum*, *C. pauciret. = Cladopyxidium paucireticulatum*, *P. tu. = Pervosphaeridium tubuloaculatum*, *D. ga. = Deflandrea galeata*, *P. de. = Palaeocystodinium denticulatum*, *H. bor. = Hystrichostrogylon borisii*, *H. co. = Hystrichostrogylon coninckii*, *gr./gr. = grimmensis/granulosus*, *la. = lanceolata*, *c. = cimbrica*, *f. = fastigata*, *teg./jun. = tegulatus/junior*, *d. = danica*, *b./d. = baltica/danica. P. ha. = Plummerita hantkeninoides*.

rence (HO) of the nannofossil marker taxon *Reinhardtites anthophorus* at the top of the Zeven Wegen Mb. at Hallembaye (Robaszynski et al. 1985) constrains the studied part of this member to the basal part of CMBE-2. The basal part of the Vijlen Mb. is marked by the HO of the nannofossil marker taxon *Tranolithus orionatus* (Robazynski et al. 1985). It is characterized by fluctuating carbon isotope values, reaching a minimum (~1.50‰) in the middle of the member. This interval correlates with nannofossil zones UC17/18 (Robaszynski et al. 1985) and the *Pervosphaeridium tubuloaculeatum* dinocyst Zone (Slimani 2000), indicating that the Vijlen Mb. at Hallembaye comprises carbon-isotope events M2+ and M2- of Thibault et al. (2012a). The last occurrence of the true (i. e., non-tegulated) inoceramids occurs at the top of the Vijlen Mb. (Walaszcyk et al. 2010), above carbon isotope event M2-, similar to the Gubbio basin (Chauris et al. 1998). From the overlying upper part of the Gulpen Fm. and superimposed Maastricht Fm., two species of tegulated inoceramid are known. *Spyridoceramus tegulatus* ranges from the Vijlen Mb. (co-occurring with true inoceramids) to the top of the Nekum Mb., while *Tenuipteria argentea* is confined to the upper Meerssen Mb. and overlying lowest Danian subunit IVf-7 of this unit (Jagt and Jagt-Yazykova 2018).

From the upper part of the Vijlen Mb. to the base of the Lixhe 2 Mb., there is an increasing trend, of about 0.25‰, followed by stable values around 1.95‰, corresponding to carbon isotope event M3+ of Thibault et al. (2012a). The HO of the nannofossil marker *Calculites obscurus* occurs in the middle of the Lixhe 1 Mb. (Robaszynski et al. 1985). The HO of this taxon differs slightly between different Boreal sections. It is recorded within M2- in Stevns-1 and within M3+ in Rørdal-1 (Thibault et al. 2012a). The overlying interval with ~0.2–0.3 permille negative excursions, in the top part of the Lixhe 2 Mb., corresponds to carbon isotope event M3-(a) of Thibault et al. (2012a), i. e., the Mid-Maastrichtian Event (MME). This is the first time the MME is recorded in the Maastrichtian type area. Based on the carbon isotope records of Gubbio (Italy), Stevns-1 (Denmark) and Hemmoor (Germany), Voigt et al. (2012) subdivided the MME into three carbon isotope events, a lower maximum (MME-1), a negative excursion (MME-2), and an upper maximum (MME-3), which each can be recognized in the carbon isotope record of the type Maastrichtian (Fig. 5). The maximum in the middle of the Lixhe 3 Mb. marks MME-3, the top of the MME interval. The negative step above the MME appears very comparable to the record at Gubbio (Voigt et al. 2012). Slightly above this, near the top of the Lixhe 3 Mb., the Lowest Occurrence (LO) of the nannofossil marker *Lithraphidites quadratus* is documented. As already noted by Keutgen (2018), this index species appears comparatively late in the Maastrichtian type area, possibly as a result of the low resolution of the nannofossil record of the type Maastrichtian (Čepek and Moorkens 1979). The base of *L. quadratus* is recorded at the base of the MME-1 in Gubbio (Italy; Gardin et al. 2012), in MME-2 at Stevns-1 (Denmark; Sheldon et al. 2010), at the base of MME-3 at ODP Hole 1210B (tropical Pacific Ocean; Lees and Bown 2005), and above the MME in Hemmoor (Germany; McLaughlin et al. 1995), similar to the type-Maastrichtian. Hence,

the LO of *L. quadratus* is globally diachronous, perhaps by up to 700 kyrs (Voigt et al. 2012). In the middle of the Lanaye Mb., within nannofossil zone UC20a (Robaszynski et al. 1985), relatively close to the LOs of the dinocyst marker *Glaphyrocysta perforata* (Schiøler el al. 1997) and nannofossil marker taxon *Nephrolithus frequens* (Van Heck 1979), there is an abrupt negative 0.3 permille excursion As it occurs just above flint marker bed L10, one of the most pronounced flint beds of the type-Maastrichtian (Felder and Bosch 1998), we consider it likely that this shift represents a diagenetic feature related to infiltration of meteoric waters. Disregarding this one spike, the remainder of the Lanaye Mb. shows gradual, stepwise decreasing values. Correlating this interval of stepwise decreasing values to the carbon isotope records of Gubbio and Stevns-1 is not straightforward. We see two possible options for this interval. It appears consistent with the interval of carbon isotope event M3-(b) and the onset of event M4-(a) recorded in the Stevns-1 (Thibault et al. 2012a) and the Lägerdorf-Kronsmoor-Hemmoor records (northern Germany; Voigt et al. 2010), showing a similar stepwise decrease (option 1). Nevertheless, if the correlation based on carbon isotope curve is correct, this would mean that the HO of the dinocyst marker taxon *Triblastula untinensis* and LOs of *G. perforata* and *N. frequens* occur later in the type-Maastrichtian record than at Stevns-1, where they occur near the top of the MME. Alternatively, if the biostratigraphic markers are synchronous with the Danish records (option 2), the carbon isotope profile of the type-Maastrichtian might deviate considerably from the patterns at Gubbio, Stevns-1 and northern Germany, with the gradually decreasing values above the MME not responding to carbon isotope events M3-(b) and M4-(b). This would mean that the upper part of the Lixhe 3 and the basal Lanaye would still fall within the upper part of the MME. Either way the ~0.4‰ negative shift represented by carbon isotope event M4-(a) appears to not be fully preserved in the record of the Maastrichtian type area. This suggests that this interval is encompassed by the stratigraphic hiatus represented by the Lichtenberg Hz.

The basal part of the Maastricht Fm., correlating to nannofossils zones UC20b-d (Čepek and Moorkens 1979), is characterized by relatively positive values, likely corresponding to carbon isotope event M4+ of Thibault et al. (2012a). Subsequently, the gradual drop in values around the Schiepersberg Mb. would then correspond to carbon isotope event M4-(b) of Thibault et al. (2012a), the equivalent of KpgE-1 of Voigt et al. (2012). The base of the acme of the dinocyst marker *Palynodinium grallator*, a marker for the Late Maastrichtian Warming Event (Woelders et al. 2018, Vellekoop et al. 2019), constrains the basal part of the Nekum Mb. to carbon isotope event M5+ of Thibault et al. (2012a), referred to as KpgE-2 in Voigt et al. (2012). The $\delta^{13}C$ minimum in the Nekum Mb can possibly be correlated with the $\delta^{13}C$ minimum between KpgE-2 and 3. This event is well constrained from open ocean records, e. g., at Walvis Ridge IODP Site 1262 (Barnet et al. 2018), where it correspond with a latest Maastrichtian warming event, consistent with the position of the *P. grallator* acme in the type-Maastrichtian record. Although the age of KpgE-1 (~66.52 Ma) used in this study following the age models of Batenburg et al. (2018) agrees well between Walvis Ridge (Barnet et al. 2018) and Zumaia (Batenburg et al. 2014), we note that it is slightly older compared to similar studies carried out in Gubbio (Sinnesael et al. 2016; 2019) and the Gulf Coastal Plain (Naujokaitytė et al. 2021) that suggest an age closer to 66.4 Ma. The interval of the Maastricht Fm. that is not represented in this study, the Meerssen Mb., would then correlate to carbon isotope event KpgE-3 of Voigt et al. (2012).

5.3. Implications of the new age model

Our new chemostratigraphic framework enables us to refine the age-model for the studied strata (Table 1). Most notable are the new ages bracketing the Froidmont Hz. at Hallembaye. The top of the Zeven Wegen Mb. is now calibrated to ~72.6 Ma, while the base of the Vijlen Mb. is updated to ~70.4 Ma, slightly older than the estimated age (69.7 Ma) in the preliminary cyclostratigraphic age model of Keutgen (2018). Hence, our updated age model indicates that the Froidmont Hz. at the Hallembaye quarry represents a stratigraphic hiatus of ~2.2 million years. The Boirs Hz. marks the main carbon-isotope excursion of the MME, dated at ~68.6 Ma, in accordance with the age model proposed by Keutgen (2018). According to our new age model, the top of the Lanaye Mb. at the former ENCI quarry is either dated at ~67.3 Ma (option 1) or at 67.7 Ma (option 2), as highlighted in the age-depth model for our record (Fig. 6). The base of the Valkenburg Mb. equates to ~67.0 Ma, albeit with a relatively large (~0.2 Myr) uncertainty, because of the limited occurrence of biostratigraphic events in the basal part of the Maastricht Fm. The Lichtenberg Hz. in the former ENCI quarry therefore represents a stratigraphic hiatus of ~0.7 mil-

Table 1. New chemostratigraphic age model for the type-Maastrichtian, compared to ages of the preliminary age model of Keutgen (2018). Ages in italics are based on interpolation. Uncertainty indicated is total uncertainty based on correlation with biostratigraphy and carbon isotope events.

Level	Stratigraphic height (mch)	Age (Ma) Keutgen 2018	Age (Ma) present study		Estimated uncertainty (myr)	Markers
Berg & Terblijt Hz.	–	66.02	66.02		0.01	K/Pg boundary
Caster Hz.	–	66.2	*(66.15)*		*(0.05)*	–interpolation-
Kanne Hz.	98.2	66.3	66.25		0.05	base *P. grallator* acme
Laumont Hz.	91.4	66.4	66.35		0.05	inflection point carbon isotope curve (M5+)
Lava Hz.	87.0	66.5	*66.4*		*0.05*	–interpolation-
Romontbos Hz.	83.0		66.55		0.05	inflection point carbon isotope curve (top M4-(b)
Schiepersberg Hz.	80.5	66.6	66.60		0.05	inflection point carbon isotope curve (base M4-(b)
mid-Gronsveld	77.0		66.70		0.05	positive carbon isotope excursion (M4+)
St. Pieter Hz.	74.0	66.7	*66.90*		*0.1*	–interpolation-
base Valkenburg (ENCI)	71.7	66.8	67.0		0.2	inflection point carbon isotope curve (base M4+)
top Lanaye (ENCI)	71.7	67.5	Opt. 1	Opt. 2	0.2	positive carbon isotope excursion (?top M3-b)
			67.3	67.7		
Lanaye L10	64.0		Opt. 1	Opt. 2	0.1	negative carbon isotope excursion (?M3-b), LO *T. utinensis*, FO *G. perforata*
			67.6	68.0		
Nivelle Hz.	57.8	68.2	Opt. 1	Opt. 2	*0.1*	–interpolation-
			67.8	*68.2*		
mid-Lixhe 3	53.0		Opt. 1	Opt. 2	0.05	inflection point carbon isotope curve (top M3-a)
			68.0	69.0		
Boirs Hz.	46.7	68.6	68.6		0.05	negative carbon isotope excursion (M3-a)
mid-Lixhe 2	42.0		*69.0*		*0.1*	–interpolation-
Hallembaye I Hz.	34.4	68.9	69.2		0.1	inflection point carbon isotope curve (top M3+)
mid-Lixhe 1	32.0		69.5		0.1	~LO *C. obscurus*
Lixhe 1 Hz.	28.0	69.2	*69.7*		*0.1*	-interpolation-
"Zonneberg Hz." (= base Vijlen +4 m) (ENCI)	15.5	69.6	69.90		0.05	FO *F. tubulosa*, FO *Triblastula wilsonii*
base Vijlen (Hallembaye)	11,75	69.7	70.4		0.1	FO *B. junior*, FO *P. neubergicus*
top Zeven Wegen	11.75		72.60		0.05	LO *Reinhardtites anthophorus*
top Zeven Wegen –6 m	5.7		72.90		0.05	inflection point carbon isotope curve (top CMBE-1). ~FO of *A. coronata, A. senonensis, A. microreticulata, N. glabrum, O. streeli, P. grallator, R. punctulum*

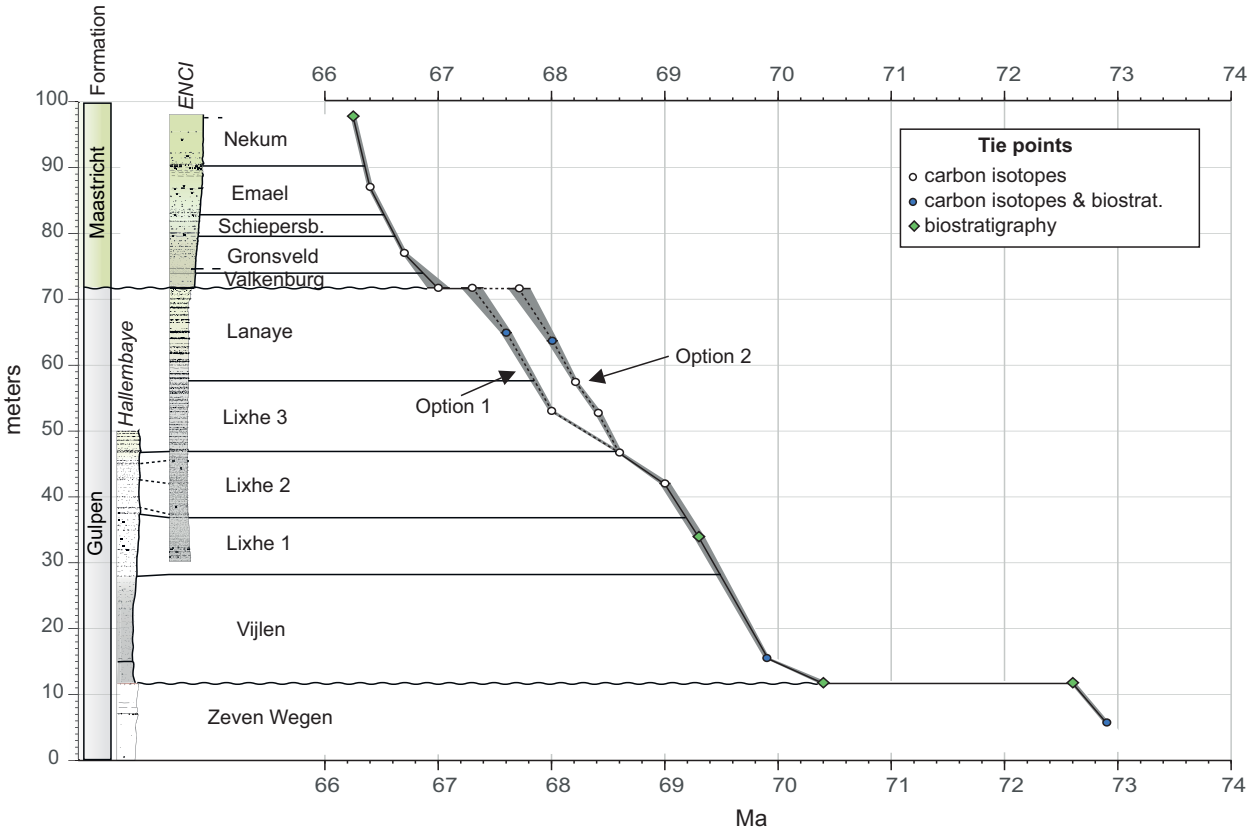

Fig. 6. Age-depth model for the type-Maastrichtian. For the upper Lixhe 3 and Lanaye, two options are considered: option 1, primarily based on the isotope stratigraphy, and option 2, based on the biostratigraphy and isotope stratigraphy.

lion years (option 2), approximately in accordance with the age model proposed by Keutgen (2018), or ~0.3 million years (option 1), considerably less than the previous estimate. For most of the Maastricht Fm., both age models (Keutgen 2018 and this study) agree relatively well (Table 1). Based on the positive carbon-isotope peak close to the Laumont and Kanne horizons, correlating to carbon isotope event M5+, and the base of the acme of the dinocyst marker *Palynodinium grallator* at the Kanne Hz., we estimate the age of this horizon to equate to ~66.3 Ma, consistent with the estimated age in the preliminary cyclostratigraphic age model by Keutgen (2018). Overall, this refined age-model yields average sedimentation rates of ~1.9 cm/kyr for the Gulpen Fm., similar to those for the Maastrichtian chalk successions of Kronsmoor/Hemmoor in northern Germany (Voigt and Schönfeld 2010, Engelke et al. 2018). The Maastricht Fm. is characterized by slightly higher average sedimentation rates, of ~3.5 cm/kyr, which matches the more proximal depositional setting, as is illustrated by abundant macroinvertebrate taxa. With an estimated age of ~66.3 Ma for the Kanne Hz., the part of the Maastricht Fm. that is not included in our profile (i. e., the top of the Nekum Mb. and overlying Meerssen Mb.) is characterized by considerably higher average sedimentation rates. With >15 m of stratigraphy (Schiøler et al. 1997) deposited in about 300 kyrs, this interval reflects average sedimentation rates of >5.0 cm/kyr, consistent with the sedimentology of very coarse-grained calcarenites and calcirudites (Felder and Bosch 2000), illustrating very shallow-marine, platform conditions characterized by high carbonate production.

The new age model presented here also allows a much-improved dating of the paleontological records from the type-Maastrichtian (Fig. 2), placing them in a global context. For example, based on the new age model, the recently published earliest known crown bird to date, *Asteriornis maastrichtensis* (Field et al. 2020), originating from the Valkenburg Member, is dated at 66.8–67.2 Ma, even older than originally presumed (66.7–66.8 Ma).

5.4. CMBE and MME

The present study is the first to recognize the characteristic Campanian–Maastrichtian Boundary Event (CMBE) and the Mid-Maastrichtian Event (MME) in the Maastrichtian type area (Fig. 5). While the top of the Zeven Wegen Mb. comprises the lowermost part of the CMBE (CMBE-1 and CMBE-2), a large part of the event (CMBE-3 to CMBE-5) is encompassed by the ~2.2 Myr stratigraphic hiatus represented by the Froidmont Horizon. The μXRF-based element profiles through the type-Maastrichtian succession suggest that this horizon represents a sequence boundary, with the stratigraphic hiatus reflecting non-deposition or erosion during regressive and lowstand phases. Worldwide, the Campanian–Maastrichtian boundary appears to be correlated to a sea level lowstand (Miller et al. 1999, Jarvis et al. 2002, Wilmsen et al. 2019), potentially linked to glacio-eustasy and/or thermal contraction of the water column due to global cooling (Miller et al. 2005). The negative $\delta^{13}C$ excursions across the CMBE might have been a direct result of this eustatic sea-level fall, enhancing lowland erosion and organic-matter oxidation (Jarvis et al. 2002). Others have argued that the time span of the CMBE is too long to explain the carbon-cycle change solely by glacio-eustasy (Voigt et al. 2012), with short-term $\delta^{13}C$ events (CMBE-1 to CMBE-5) probably linked to orbitally forced climate changes, occurring superimposed on long-term shifts in the carbon cycle driven by large-scale processes such as changes in plate-tectonic configuration, mid-ocean ridge subduction or hot-spot volcanism (Coffin et al. 2002, Müller et al. 2008).

The MME in the Maastrichtian type area, which is situated around the transition between the Lixhe 2 and Lixhe 3 Members, is characterized by a lower maximum (MME-1), several ~0.2–0.3 permille negative carbon isotope excursions (MME-2) and an upper maximum (MME-3). This upper maximum shows the most positive isotopic value of the Maastrichtian part of the record. While it has been suggested that the enigmatic extinction of the inoceramid bivalves might be related to the MME (MacLeod et al. 1996, Frank et al. 2005, Jung et al. 2013), the true (i. e., non-tegulated) inoceramids disappear earlier in the type-Maastrichtian record. Here, they disappear at the top of the Vijlen Mb. (Walaszcyk et al. 2010), above carbon isotope event M2-, dating the extinction of the true inoceramids in the Maastrichtian type area at ~69.5 Ma. It has been argued that the extinction of non-tegulated inoceramids was diachronous across the world, occurring at ~69.6 Ma in the Gubbio record (Chauris et al. 1998), at ~69.3 Ma in the Basque region (Spain and France; see Gómez-Alday et al. 2004, Batenburg et al. 2014), at 68.6–68.9 Ma in the northwest Pacific (Frank et al. 2005) and at 68.5–68.7 Ma in the western North Atlantic (MacLeod and Huber 2001, Huber et al. 2008). Some authors have suggested that non-tegulated inoceramids disappeared earlier in high-latitude and shallow-marine sites (MacLeod et al. 1996). The relatively early extinction of true inoceramids at ~69.5 Ma in the shallow-marine, boreal-influenced type-Maastrichtian area is consistent with this hypothesis.

6. Conclusions

The new carbonate stable carbon-isotope record of the Maastrichtian type area shows a strong resemblance to the astronomically calibrated isotope records from Gubbio, Italy, and other records in Europe, such as Stevns-1 in Denmark, allowing a regional and global correlation. Key carbon-isotope events, such as the Campanian–Maastrichtian Boundary Event (CMBE) and the Mid-Maastrichtian Event (MME) are recognized in the ~98 m thick type-Maastrichtian record from the Hallembaye and former ENCI quarries. Micro-XRF analysis revealed variable terrigenous input over time, in the type-Maastrichtian carbonate paleoenvironment. Three distinct stratigraphic sequences are recognized, each characterized by an upward trend of increasingly more pure carbonates, separated by sequence boundaries at the Froidmont, Lichtenberg and Vroenhoven horizons. Our refined age model provides estimates for the time encompassed by the stratigraphic hiatuses in the succession. The Froidmont Horizon represents a stratigraphic hiatus of ~2.2 Myr, while the Lichtenberg Horizon represents approximately 0.3–0.7 Myr. The new chemostratigraphic framework, integrated with key biostratigraphic makers, presented here provides additional paleoenvironmental context for the type-Maastrichtian strata and fossils and enables us to refine their chronostratigraphy. This age model allows us to place the unique paleontological records from the type-Maastrichtian in a global context for the first time.

Acknowledgements. We are thankful to Silke Voigt and Sietske Batenburg for their insightful comments and suggestions, significantly improving this manuscript. Furthermore, we wish to thank Kreco BV, ENCI-HeidelbergCe-

ment Group and Natuurmonumenten for providing access to the Hallembaye and former ENCI quarries. We are grateful to Anthonie Hellemond, Kevin Nolis, Flore van Maldeghem, Michiel Arts, Anne-Christine da Silva, Sander Hilgen, Monika Doubrawa, Alexander Clark, Iris Vancoppenolle, Hannah van der Geest, Joep Schaeffer and Eric Nieuwenhuis for their help with the sampling campaigns in both quarries. We also thank Mauri Rosiers, Houceine El Mir, Tom Clarys, Jochen Pedro Eeckhoudt, Kiano Gorissen, Tom Gaston Hamelryck and Robin Francotte for preparing samples for μXRF and stable isotope analysis. This work was funded by grants 12Z6621N (to JV) and 11E6621N (to PK) of the Research Foundation Flanders (FWO). PC thanks the FWO – Hercules Program for financing the μXRF instrument and the Nu-Perspective IRMS at the VUB. The support of the VUB Strategic Research program is also acknowledged.

Barnet, J. S. K., Littler, K., Kroon, D., Leng, M. L., Westerhold, T., Röhl, U., Zachos, J. C., 2018. A new high-resolution chronology for the late Maastrichtian warming event: Establishing robust temporal links with the onset of Deccan volcanism. Geology 46 (2), 147–150, https://doi.org/10.1130/G39771.1.

Bastiaans, D., Kroll, J. J. F., Cornelissen, D., Jagt, J. W. M., Schulp, A. S., 2020. Cranial palaeopathologies in a Late Cretaceous mosasaur from the Netherlands. Cretaceous Research 112, 104425, https://doi.org/10.1016/j.cretres.2020.104425.

Batenburg, S. J., Friedrich, O., Moriya, K., Voigt, S., Cournède, C., Blum, P., …, Wilson, P. A., 2018. Late Maastrichtian carbon isotope stratigraphy and cyclostratigraphy of the Newfoundland Margin (Site U1403, IODP Leg 342). Newsletters on Stratigraphy 51 (2), 245–260, https://doi.org/10.1127/nos/2017/0398.

Batenburg, S. J., Gale, A. S., Sprovieri, M., Hilgen, F. J., Thibault, N., Boussaha, M., Orue-Etxebarria, X., 2014. An astronomical time scale for the Maastrichtian based on the Zumaia and Sopelana sections (Basque country, northern Spain). Journal of the Geological Society 171 (2), 165–180, https://doi.org/10.1144/jgs2013-015.

Burnett, J., 1990. A new nannofossil zonation scheme for the Boreal Campanian. INA Newsletter 12 (3), 67–70.

Čepek, P., Moorkens, T., 1979. Cretaceous/Tertiary boundary and Maastrichtian-Danian biostratigraphy (Coccoliths and Foraminifera) in the Maastrichtian type area. In: Christensen, W. K., Birkelund, T. (Eds.), Proceedings of the Symposium on Cretaceous-Tertiary Boundary Events, II, pp. 137–142, Copenhagen, University of Copenhagen Press.

Chauris, H., LeRousseau, J., Beaudoin, B., Propson, S., Montanari, A., 1998. Inoceramid extinction in the Gubbio basin (northeastern Apennines of Italy) and relations with mid-Maastrichtian environmental changes. Palaeogeography, Palaeoclimatology, Palaeoecology 139 (3–4), 177–193, https://doi.org/10.1016/S0031-0182(97)00150-8.

Christensen, W. K., Hancock, J. M., Peake, N. B., Kennedy, W. J., 2000. The base of the Maastrichtian. Bulletin of the Geological Society of Denmark 47, 81–85.

Coffin, M. F., Pringle, M. S., Duncan, R. A., Gladczenko, T. P., Storey, M., Muller, R. D., Gahagan, L. A., 2002. Kerguelen Hotspot magma output since 130 Ma. Journal of Petrology 43 (7), 1121–1137, https://doi.org/10.1093/petrology/43.7.1121.

Conybeare, W. D., 1822. Fossil crocodiles and other saurian animals.. In: Parkinson, J. (Ed.), Outlines of oryctology. An introduction to the study of fossil organic remains; especially of those found in the British strata: intended to aid the student in his enquiries respecting the nature of fossils and their connection with the formation of the earth, pp. vii + 344, London, Sherwood, Neely and Jones/W. Phillips.

Dameron, S. N., Leckie, R. M., Clark, K., MacLeod, K. G., Thomas, D. J., Lees, J. A., 2017. Extinction, dissolution, and possible ocean acidification prior to the Cretaceous/Paleogene (K/Pg) boundary in the tropical Pacific. Palaeogeography, Palaeoclimatology, Palaeoecology 485, 433–454, https://doi.org/10.1016/j.palaeo.2017.06.032.

De Winter, N. J., Claeys, P., 2017. Micro X-ray fluorescence (μXRF) line scanning on Cretaceous rudist bivalves: A new method for reproducible trace element profiles in bivalve calcite. Sedimentology 64 (1), 231–251, https://doi.org/10.1111/sed.12299.

De Winter, N. J., Dämmer, K., Falkenroth, M., Reichart, G.-J., Moretti, S., Martínez-García, A., …, Ziegler, M., 2021. Multi-isotopic and trace element evidence against different formation pathways for oyster microstructures. Geochimica et Cosmochimica Acta 308, 326–352, https://doi.org/10.1016/j.gca.2021.06.012.

De Winter, N. J., Sinnesael, M., Makarona, C., Vansteenberge, S., Claeys, P., 2017. Trace element analyses of carbonates using portable and micro-X-ray fluorescence: Performance and optimization of measurement parameters and strategies. Journal of Analytical Atomic Spectrometry 32 (6), 1211–1223, https://doi.org/10.1039/C6JA00361C.

Donovan, S. K., Jagt, J. W. M., 2013. Aspects of clavate borings in the type Maastrichtian (Upper Cretaceous) of the Netherlands and Belgium. In: Mulder, E. W. A., Jagt, J. W. M., Schulp, A. S. (Eds.), The Sunday's child of Dutch earth sciences – a tribute to Bert Boekschoten on the occasion of his 80th birthday. Netherlands Journal of Geosciences, 92, 133–143, https://doi.org/10.1017/S0016774600000068.

Dortangs, R. W., Schulp, A. S., Mulder, E. W. A., Jagt, J. W. M., Peeters, H. H. G., De Graaf, D. T., 2002. A large new mosasaur from the Upper Cretaceous of The Netherlands. Netherlands Journal of Geosciences 81 (1), 1–8, https://doi.org/10.1017/S0016774600020515.

Eldrett, J. S., Vieira, M., Gallagher, L., Hampton, M., Blaauw, M., Swart, P. K., 2021. Late Cretaceous to Palaeogene carbon isotope, calcareous nannofossil and foraminifera stratigraphy of the Chalk Group, Central North Sea. Marine and Petroleum Geology 124, 104789, https://doi.org/10.1016/j.marpetgeo.2020.104789.

Engelke, J., Linnert, C., Niebuhr, B., Schnetger, B., Brumsack, H.-J., Mutterlose, J., Wilmsen, M., 2018. Tracking Late Cretaceous environmental change: Geochemical environment of the upper Campanian to lower Maastrichtian chalks at Kronsmoor, northern Germany. Cretaceous Research 84, 323–339, https://doi.org/10.1016/j.cretres.2017.10.001.

Felder, P. J., 2001. Bioklasten-stratigrafie of ecozonatie voor het krijt (Santoniaan–Campaniaan–Maastrichtiaan) van Zuid-Limburg en oostelijk België. Memoirs of the Geological Survey of Belgium 47, 1–141.

Felder, P. J., Bless, M. J. M., 1994. The Vijlen Chalk (early Early to early Late Maastrichtian) in its type area around Vijlen and Mamelis (southern Limburg, The Netherlands). Annales de la Société géologique de Belgique 116 (for 1993), 61–85.

Felder, P. J., Keppens, E., Declercq, B., Normand, S., Streel, M., 2003. Faunal/floral and isotopic responses to Milankovitch precession cycles and environmental changes in the upper Gulpen Formation (Upper Maastrichtian) at the CBR-Lixhe and ENCI-Maastricht bv quarries. In: Jagt, J. W. M., Schulp, A. S., De Graaf, D. Th. (Eds.), The 150th anniversary of the Maastrichtian Stage – a celebratory conference. Netherlands Journal of Geosciences 82, 275–281.

Felder, W. M., 1975. Lithostratigrafie van het Boven-Krijt en het Dano-Montien in Zuid-Limburg en het aangrenzende gebied. In: Zagwijn, W. H., Van Staalduinen, C. J. (Eds.), Toelichting bij geologische overzichtskaarten van Nederland, pp. 63–72, Haarlem, Rijks Geologische Dienst.

Felder, W. M., Bosch, P. W., 1998. Geologie van de St. Pietersberg bij Maastricht. Grondboor & Hamer 52, 53–63.

Felder, W. M., Bosch, P. W., 2000. Geologie van Nederland, deel 5, Delft, Utrecht, Krijt van Zuid-Limburg. Nederlands Instituut voor Toegepaste Geowetenschappen TNO.

Field, D. J., Benito, J., Chen, A., Jagt, J. W. M., Ksepka, D. T., 2020. Late Cretaceous neornithine from Europe illuminates the origins of crown birds. Nature 579 (7799), 397–401, https://doi.org/10.1038/s41586-020-2096-0.

Frank, T. D., Thomas, D. J., Leckie, M., Arthur, M. A., Bown, P. R., Jones, K., Lees, J. A., 2005. The Maastrichtian record from Shatsky Rise (northwest Pacific): A tropical perspective on global ecological and oceanographic changes. Paleoceanography 20 (1), 1–14, https://doi.org/10.1029/2004PA001052.

Gale, A. S., Mutterlose, J., Batenburg, S., 2020. The Cretaceous Period. In: Gradstein, F. M., Ogg, J. G., Schmitz, M. D., Ogg, G. M. (Eds.), Geologic Time Scale 2020, pp. 1023–1086, Amsterdam, The Netherlands, Elsevier BV, https://doi.org/10.1016/B978-0-12-824360-2.00027-9.

Gardin, S., Galbrun, B., Thibault, N., Coccioni, R., Silva, I. P., 2012. Bio-magnetochronology for the upper Campanian-Maastrichtian from the Gubbio area, Italy: New results from the Contessa Highway and Bottaccione sections. Newsletters on Stratigraphy 45 (1), 75–103, https://doi.org/10.1127/0078-0421/2012/0014.

Gómez-Alday, J. J., López, G., Elorza, J., 2004. Evidence of climatic cooling at the Early/Late Maastrichtian boundary from inoceramid distribution and isotopes: Sopelana sections, Basque Country, Spain. Cretaceous Research 25 (5), 649–668, https://doi.org/10.1016/j.cretres.2004.06.009.

Grabau, A. W., 1904. On the classification of sedimentary rocks. American Geologist 33, 228–247.

Huber, B. T., MacLeod, K. G., Tur, N. A., 2008. Chronostratigraphic framework for Upper Campanian-Maastrichtian sediments on the Blake Nose (subtropical North Atlantic). Journal of Foraminiferal Research 38 (2), 162–182, https://doi.org/10.2113/gsjfr.38.2.162.

Jagt, J. W. M., Collins, J. S. H., 1999. Log-associated late Maastrichtian cirripedes from northeast Belgium. Palaontologische Zeitschrift 73 (1–2), 99–111, https://doi.org/10.1007/BF02987985.

Jagt, J. W. M., 2001. The historical stratotype of the Maastrichtian: a review. In: Odin, G. S. (Ed.), The Campanian-Maastrichtian stage boundary. Characterisation at Tercis les Bains (France) and correlation with Europe and other continents, [Developments in Palaeontology and Stratigraphy, 19], pp. 63–72, Amsterdam, Elsevier.

Jagt, J. W. M., 2015. Les fossiles néocrétacés de la region de Maastricht (Pays-Bas, Belgique). Fossiles, Revue française de paléontologie 24, 39–71.

Jagt, J. W. M., Jagt-Yazykova, E. A., 2012. Stratigraphy of the type-Maastrichtian – a synthesis. In: Jagt, J. W. M., Donovan, S. K., Jagt-Yazykova, E. A. (Eds.), Fossils of the type Maastrichtian (Part 1). Scripta Geologica Special Issue, 8, 5–32.

Jagt, J. W. M., Jagt-Yazykova, E. A., 2016. The Upper Cretaceous and lower Paleogene in the type area of the Maastrichtian stage (72.1–66 Ma) – Field guide. European Association of Vertebrate Palaeontologists, 14th Annual Meeting, Teylers Museum, Haarlem (the Netherlands), 6–10 July 2016, 18 p.

Jagt, J. W. M., Jagt-Yazykova, E. A., 2018. Stratigraphical ranges of tegulated inoceramid bivalves in the type area of the Maastrichtian Stage (Belgium, the Netherlands). In: Jagt-Yazykova, E. A., Jagt, J. W. M., Mortimore, R. N. (Eds.), Advances in Cretaceous palaeontology and stratigraphy – Christopher John Wood Memorial Volume. Cretaceous Research, 87, 385–394, https://doi.org/10.1016/j.cretres.2017.05.022

Jagt, J. W. M., Donovan, S. K., Fraaije, R., Mulder, E. W. A., Nieuwenhuis, E., Stroucken, J., …, Van Knippenberg, P., 2015. Remarkable preservation of selected latest Cretaceous macrofossils from the Maastrichtian type area (the Netherlands, Belgium). In: Sullivan, R. M., Lucas, S. G. (Eds.), Fossil Record 4. New Mexico Museum of Natural History and Science Bulletin, 67, 75–78

Jagt, J. W. M., Mulder, E. W. A., Schulp, A. S., Dortangs, R. W., Fraaije, R. H. B., 2003. Dinosaurs from the Maastrichtian-type area (southeastern Netherlands, northeastern Belgium). Comptes Rendus. Palévol 2 (1), 67–76, https://doi.org/10.1016/S1631-0683(03)00004-6.

Jarvis, I., 1992. Sedimentology, geochemistry and origin of phosphatic chalks: The Upper Cretaceous deposits of NW Europe. Sedimentology 39 (1), 55–97, https://doi.org/10.1111/j.1365-3091.1992.tb01023.x.

Jarvis, I., Mabrouk, A., Moody, R. T. J., de Cabrera, S., 2002. Late Cretaceous (Campanian) carbon isotope events, sea-level change and correlation of the Tethyan and Boreal realms. Palaeogeography, Palaeoclimatology, Palaeoecology 188 (3–4), 215–248, https://doi.org/10.1016/S0031-0182(02)00578-3.

Jarvis, I., Murphy, A. M., Gale, A. S., 2001. Geochemistry of pelagic and hemipelagic carbonates: Criteria for identifying systems tracts and sea-level change. Journal of the Geological Society 158 (4), 685–696, https://doi.org/10.1144/jgs.158.4.685.

Jenkyns, H. C., Mutterlose, J., Sliter, W. V., 1995. Upper Cretaceous carbon- and oxygen-isotope stratigraphy of deep-water sediments from the North-Central Pacific (Site 869, flank of Pikini-Wodejebato, Marshall Islands). Proceedings of the Ocean Drilling Program, Scientific Results 143, 105–108.

Jung, C., Voigt, S., Friedrich, O., Koch, M. C., Frank, M., 2013. Campanian-Maastrichtian ocean circulation in the tropical Pacific. Paleoceanography 28 (3), 562–573, https://doi.org/10.1002/palo.20051.

Kaskes, P., Brunke, L., Emaus, R., Bastiaans, D., Schulp, A. S., 2017. A novel 3D visualization of dinosaur bonebeds: Integrating geology, paleontology and archaeology. Geological Society of America Abstracts with Programs 49 (6), 306574, https://doi.org/10.1130/abs/2017AM-306574.

Kaskes, P., Déhais, T., de Graaff, S. J., Goderis, S., Claeys, P., 2021. Micro-X-ray fluorescence (μXRF) analysis of proximal impactites: high-resolution element mapping, digital image analysis, and quantifications. In: Reimold, W. U., Koeberl, C. (Eds.), Geological Society of America, Special Paper 550, Large meteorite impacts and planetary evolution VI, pp. 171–206, https://doi.org/10.1130/2021.2550(07).

Keutgen, N., 2018. A bioclast-based astronomical timescale for the Maastrichtian in the type area (southeast Netherlands, northeast Belgium) and stratigraphic implications: The legacy of P. J. Felder. Netherlands Journal of Geosciences 97 (4), 229–260, https://doi.org/10.1017/njg.2018.15.

Keutgen, N., Jagt, J. W. M., 1998. Late Campanian belemnite faunas from Liège-Limburg (NE Belgium, SE Netherlands). Geological Survey of Belgium, Professional Paper 1998/2 (287), 1–32.

Keutgen, N., Jagt, J. W. M., 2009. Correlation of Maastrichtian strata in the southeast Netherlands and adjacent regions, northern Germany, northern Spain and the USA. Byulleten' Moskovskogo Obshchestva Ispytatelej Prirody. Otdel Geologicheskii 84, 71–77.

Keutgen, N., Jagt, J. W. M., Felder, P. J., Jagt-Yazykova, E., 2010. Stratigraphy of the upper Vijlen Member (Gulpen Formation; Maastrichtian) in northeast Belgium, the southeast Netherlands and the Aachen area (Germany), with special reference to belemnitellid cephalopods. Netherlands Journal of Geosciences 89 (2), 109–136, https://doi.org/10.1017/S0016774600000731.

Lees, J. A., Bown, P. R., 2005. Upper Cretaceous calcareous nannofossil biostratigraphy, ODP Leg 198 (Shatsky Rise, northwest Pacific Ocean). In: Bralower, T. J., Premoli Silva, I., Malone, M. J. (Eds.), Proceedings of the Ocean Drilling Program, Scientific Results, College Station, TX, 1–60.

Leriche, M., 1929. Les poissons du Crétacé marin de la Belgique et du Limbourg hollandais (Note préliminaire). Les résultats stratigraphiques de leur étude. Bulletin de la Société belge de Géologie, de Paléontologie et d'Hydrologie 37, 199–299.

Leys, C., Ley, C., Klein, O., Bernard, P., Licata, L., 2013. Detecting outliers: Do not use standard deviation around the mean, use absolute deviation around the median. Journal of Experimental Social Psychology 49 (4), 764–766, https://doi.org/10.1016/j.jesp.2013.03.013.

MacLeod, K. G., 1994. Bioturbation, inoceramid extinction and mid-Maastrichtian ecological change. Geology 22 (2), 139–142, https://doi.org/10.1130/0091-7613(1994)022<0139:BIEAMM>2.3.CO;2.

MacLeod, K. G., Huber, B. T., 2001. The Maastrichtian record at Blake Nose (western North Atlantic) and implications for global palaeoceanographic and biotic changes. In: Kroon, D., Norris, R. D., Klaus, A. (Eds.), Geological Society, London, Special Publications 183, Western North Atlantic Palaeogene and Cretaceous palaeoceanography, pp. 111–130, https://doi.org/10.1144/GSL.SP.2001.183.01.06.

MacLeod, K. G., Huber, B. T., Ward, P. D., 1996. The biostratigraphy and paleobiogeography of Maastrichtian inoceramids. In: Ryder, G., Fastovsky, D., Gartner, S. (Eds.), Geological Society of America, Special Paper 307, The Cretaceous-Tertiary event and other catastrophes in earth history, pp. 361–373.

Madzia, D., Jagt, J. W. M., Mulder, E. W. A., 2020. Osteology, phylogenetic affinities and taxonomic status of the enigmatic late Maastrichtian ornithopod taxon *Orthomerus dolloi* (Dinosauria, Ornithischia). Cretaceous Research 108, 104334, https://doi.org/10.1016/j.cretres.2019.104334.

Martin, J. E., Case, J. A., Jagt, J. W. M., Schulp, A. S., Mulder, E. W. A., 2005. A new European marsupial indicates a Late Cretaceous high-latitude transatlantic dispersal route. Journal of Mammalian Evolution 12 (3–4), 495–511, https://doi.org/10.1007/s10914-005-7330-x.

Mateo, P., Keller, G., Punekar, J., Spangenberg, J. E., 2017. Early to Late Maastrichtian environmental changes in the Indian Ocean compared with Tethys and South Atlantic. Palaeogeography, Palaeoclimatology, Palaeoecology 478, 121–138, https://doi.org/10.1016/j.palaeo.2017.01.027.

McLaughlin, O. M., McArthur, J. M., Thirlwall, M. F., Howarth, R., Burnett, J., Gale, A. S., Kennedy, W. J., 1995. Sr isotope evolution of Maastrichtian seawater, deter-

mined from the Chalk of Hemmoor, NW Germany. Terra Nova 7 (5), 491–499, https://doi.org/10.1111/j.1365-3121.1995.tb00550.x.

Miller, K. G., Barrera, E., Olsson, R. K., Sugarman, P. J., Savin, S. M., 1999. Does ice drive early Maastrichtian eustasy? Geology 27 (9), 783–786, https://doi.org/10.1130/0091-7613(1999)027<0783:DIDEME>2.3.CO;2.

Miller, K. G., Wright, J. D., Browning, J. V., 2005. Vision of ice sheets in a greenhouse world. Marine Geology 217 (3–4), 215–231, https://doi.org/10.1016/j.margeo.2005.02.007.

Mitchell, S. F., Ball, J. D., Crowley, S. F., Marshall, J. D., Paul, C. R. C., Veltkamp, C. J., Samir, A., 1997. Isotope data from Cretaceous chalks and foraminifera: Environmental or diagenetic signals? Geology 25 (8), 691–694, https://doi.org/10.1130/0091-7613(1997)025<0691:IDFCCA>2.3.CO;2.

Mulder, E. W. A., Jagt, J. W. M., Kuypers, M. M. M., Peeters, H. H. G., Rompen, P., 1998. Preliminary observations on the stratigraphic distribution of Late Cretaceous marine and terrestrial reptiles from the Maastrichtian type area (SE Netherlands, NE Belgium). Oryctos 1, 55–64.

Müller, R. D., Sdrolias, M., Gaina, C., Roest, W. R., 2008. Age, spreading rates, and spreading asymmetry of the world's ocean crust. Geochemistry Geophysics Geosystems 9 (4), Q04006, https://doi.org/10.1029/2007GC001743.

Naujokaitytė, J., Garb, M. P., Thibault, N., Brophy, S. K., Landman, N. H., Witts, J. D., …, Myers, C. E., 2021. Milankovitch cyclicity in the latest Cretaceous of the Gulf Coastal Plain, USA. Sedimentary Geology 421, 105954, https://doi.org/10.1016/j.sedgeo.2021.105954.

Niebuhr, B., 2005. Geochemistry and time-series analyses of orbitally forced Upper Cretaceous marlelimestone rhythmites (Lehrte West Syncline, northern Germany). Geological Magazine 142 (1), 31–55, https://doi.org/10.1017/S0016756804009999.

Odin, G. S., Lamaurelle, M. A., 2001. The global Campanian-Maastrichtian stage boundary. Episodes 24 (4), 229–238, https://doi.org/10.18814/epiiugs/2001/v24i4/002.

Olde, K., Jarvis, I., Uličný, D., Pearce, M. A., Trabucho-Alexandre, J., Čech, S., …, Tocher, B. A., 2015. Geochemical and palynological sea-level proxies in hemipelagic sediments: A critical assessment from the Upper Cretaceous of the Czech Republic. Palaeogeography, Palaeoclimatology, Palaeoecology 435, 222–243, https://doi.org/10.1016/j.palaeo.2015.06.018.

Robaszynski, F., 1987. Biostratigraphy at the Campanian-Maastrichtian boundary. Annales de la Société géologique de Belgique 109, 325–331.

Robaszynski, F., Bless, M. J. M., Felder, P. J., Foucher, J.-C., Legoux, O., Manivit, H., …, Van der Tuuk, L. A., 1985. The Campanian-Maastrichtian boundary in the chalky facies close to the type-Maastrichtian area. Bulletin des Centres de Recherches Exploration-Production Elf-Aquitaine 9, 1–113.

Rousseeuw, P. J., Croux, C., 1993. Alternatives to the Median Absolute Deviation. Journal of the American Statistical Association 88 (424), 1273–1283, https://doi.org/10.1080/01621459.1993.10476408.

Schiøler, P., Wilson, G. J., 1993. Maastrichtian dinoflagellate zonation in the Dan Field, Danish North Sea. Review of Palaeobotany and Palynology 78 (3–4), 321–351, https://doi.org/10.1016/0034-6667(93)90070-B.

Schiøler, P., Brinkhuis, H., Roncaglia, L., Wilson, G. J., 1997. Dinoflagellate biostratigraphy and sequence stratigraphy of the Type Maastrichtian (Upper Cretaceous), ENCI Quarry, The Netherlands. Marine Micropaleontology 31 (1–2), 65–95, https://doi.org/10.1016/S0377-8398(96)00058-8.

Schrag, D. P., DePaolo, D. J., Richter, F. M., 1995. Reconstructing past sea surface temperatures: Correcting for diagenesis of bulk marine carbonate. Geochimica et Cosmochimica Acta 59 (11), 2265–2278, https://doi.org/10.1016/0016-7037(95)00105-9.

Schulz, M.-G., Ernst, G., Ernst, H., Schmid, F., 1984. Coniacian to Maastrichtian stage boundaries in the standard section for the Upper Cretaceous white chalk of NW Germany (Lägerdorf-Kronsmoor-Hemmoor): Definitions and proposals. Bulletin of the Geological Society of Denmark 33, 203–215.

Sheldon, E., Ineson, J., Bown, P., 2010. Late Maastrichtian warming in the Boreal Realm: Calcareous nannofossil evidence from Denmark. Palaeogeography, Palaeoclimatology, Palaeoecology 295 (1–2), 55–75, https://doi.org/10.1016/j.palaeo.2010.05.016.

Sinnesael, M., De Vleeschouwer, D., Coccioni, R., Claeys, P., Frontalini, F., Jovane, L., …, Montanari, A., 2016. High-resolution multiproxy cyclostratigraphic analysis of environmental and climatic events across the Cretaceous-Paleogene boundary in the classic pelagic succession of Gubbio (Italy). In: Menichetti, M., Coccioni, R., Montanari, A. (Eds.), Geological Society of America Special Paper 524, The Stratigraphic Record of Gubbio: Integrated Stratigraphy of the Late Cretaceous–Paleogene Umbria-Marche Pelagic Basin, pp. 115–137, https://doi.org/10.1130/2016.2524(09).

Sinnesael, M., De Winter, N. J., Snoeck, C., Montanari, A., Claeys, P., 2018. An integrated pelagic carbonate multiproxy study using portable X-ray fluorescence (pXRF): Maastrichtian strata from the Bottaccione Gorge, Gubbio, Italy. Cretaceous Research 91, 20–32, https://doi.org/10.1016/j.cretres.2018.04.010.

Sinnesael, M., Montanari, A., Frontalini, F., Coccioni, R., Gattacceca, J., Snoeck, C., Wegner, W., Koeberl, C., Morgan, L. E., de Winter, N. J., DePaolo, D. J., Claeys, P., 2019. Multiproxy Cretaceous–Paleogene boundary event stratigraphy.. In: Koeberl, C., Bice, D. M. (Eds.), 250 million years of earth history in central Italy: celebrating 25 years of the Geological Observatory of Coldigioco. Geological Society of America Special Paper 542, 133–158.

Slimani, H., 2000. Nouvelle zonation aux kystes de dinoflagellés du Campanien au Danien dans le nord et l'est de

la Belgique et dans le sud-est des Pays-Bas. Memoirs of the Geological Survey of Belgium 46, 1–87.

Slimani, H., Louwye, S., Dusar, M., Lagrou, D., 2011. Connecting the Chalk Group of the Campine Basin to the dinoflagellate cyst biostratigraphy of the Campanian to Danian in borehole Meer (northern Belgium). In: Jagt, J. W. M., Jagt-Yazykova, E. A., Schins, W. J. H. (Eds.), A tribute to the late Felder brothers – pioneers in Limburg geology and prehistoric archaeology. Netherlands Journal of Geosciences, 90 (2–3), 129–164, https://doi.org/10.1017/S0016774600001074.

Surlyk, F., Rasmussen, S. L., Boussaha, M., Schiøler, P., Schovsbo, N. H., Sheldon, E., …, Thibault, N., 2013. Upper Campanian-Maastrichtian holostratigraphy of the eastern Danish Basin. Cretaceous Research 46, 232–256, https://doi.org/10.1016/j.cretres.2013.08.006.

Thibault, N., Harlou, R., Schovsbo, N., Schiøler, P., Minoletti, F., Galbrun, B., …, Surlyk, F., 2012a. Upper Campanian-Maastrichtian nannofossil biostratigraphy and high-resolution carbon-isotope stratigraphy of the Danish Basin: Towards a standard δ13C curve for the Boreal Realm. Cretaceous Research 33 (1), 72–90, https://doi.org/10.1016/j.cretres.2011.09.001.

Thibault, N., Husson, D., Harlou, R., Gardin, S., Galbrun, B., Huret, E., Minoletti, F., 2012b. Astronomical calibration of upper Campanian-Maastrichtian carbon isotope events and calcareous plankton biostratigraphy in the Indian Ocean (ODP Hole 762C): Implication for the age of the Campanian-Maastrichtian boundary. Palaeogeography, Palaeoclimatology, Palaeoecology 337–338, 52–71, https://doi.org/10.1016/j.palaeo.2012.03.027.

Van der Ham, R. W. J. M., Van Konijnenburg-van Cittert, J. H. A., 2003. Rare conifers from the type area of the Maastrichtian (Upper Cretaceous, southeast Netherlands). Scripta Geologica 126, 111–119.

Van der Ham, R. W. J. M., Jagt, J. W. M., Renkens, S., Van Konijnenburg-van Cittert, J. H. A., 2010. Seed-cone scales from the upper Maastrichtian document the last occurrence in Europe of the Southern Hemisphere conifer family Araucariaceae. Palaeogeography, Palaeoclimatology, Palaeoecology 291 (3–4), 469–473, https://doi.org/10.1016/j.palaeo.2010.03.017.

Van der Ham, R. W. J. M., Van Konijnenburg-van Cittert, J. H. A., Dortangs, R. W., Herngreen, G. F. W., Van der Burgh, J., 2003. *Brachyphyllum patens* (Miquel) comb. nov. (Cheirolepidiaceae?): Remarkable conifer foliage from the Maastrichtian type area (Late Cretaceous, NE Belgium, SE Netherlands). Review of Palaeobotany and Palynology 127 (1–2), 77–97, https://doi.org/10.1016/S0034-6667(03)00095-2.

Van Heck, S. E., 1979. Nannoplankton contents of the type-Maastrichtian. International Nannoplankton Association Newsletter 1, 5–6.

Van Wagoner, J. C., Posamentier, H. W., Mitchum, R. M., Vail, P. R., Sarg, J. F., Loutit, T. S., Hardenbol, J., 1988. An overview of sequence stratigraphy and key definitions. In: Wilgus, C. K., Hastings, B. S., Kendall, C. G. St. C., Posamentier, H. W., Ross, C. A., Van Wagoner, J. C. (Eds.), Sea level changes – an integrated approach, pp. 39–45, SEPM Special Publication 42, https://doi.org/10.2110/pec.88.01.0039.

Vandenberghe, N., Van Simaeys, S., Steurbaut, E., Jagt, J. W. M., Felder, P. J., 2004. Stratigraphic architecture of the Upper Cretaceous and Cenozoic along the southern border of the North Sea Basin in Belgium. Netherlands Journal of Geosciences 83 (3), 155–171, https://doi.org/10.1017/S0016774600020229.

Vellekoop, J., 2019. The Maastrichtian Geoheritage Project: an introduction, first results and outlook, Abstract and presentation, International Symposium on Chalk &, Flint, Maastricht, the Netherlands, 30 November 2019.

Vellekoop, J., Woelders, L., Sluijs, A., Miller, K. G., Speijer, R. P., 2019. Phytoplankton community disruption caused by the latest Cretaceous global warming. Biogeosciences 16 (21), 4201–4210, https://doi.org/10.5194/bg-16-4201-2019.

Vellekoop, J., Van Tilborgh, K. H., Van Knippenberg, P., Jagt, J. W. M., Stassen, P., Goolaerts, S., Speijer, R. P., 2020. Type-Maastrichtian gastropod faunas show rapid ecosystem recovery following the Cretaceous-Palaeogene boundary catastrophe. Palaeontology 63 (2), 349–367, https://doi.org/10.1111/pala.12462.

Voigt, S., Schönfeld, J., 2010. Cyclostratigraphy of the reference section for the Cretaceous white chalk of northern Germany, Lägerdorf-Kronsmoor: A late Campanian-early Maastrichtian orbital time scale. Palaeogeography, Palaeoclimatology, Palaeoecology 287 (1–4), 67–80, https://doi.org/10.1016/j.palaeo.2010.01.017.

Voigt, S., Gale, A. S., Jung, C., Jenkyns, H. C., 2012. Global correlation of Upper Campanian-Maastrichtian successions using carbon-isotope stratigraphy: Development of a new Maastrichtian timescale. Newsletters on Stratigraphy 45 (1), 25–53, https://doi.org/10.1127/0078-0421/2012/0016.

Voigt, S., Wagreich, M., Surlyk, F., Walaszcyk, I., Ulicny, D., Cech, S., Voigt, T., Wiese, F., Wilmsen, M., Niebuhr, M., Funk, H., Michalik, J., Jagt, J. W. M., Felder, P. J., Schulp, A. S., 2008. Cretaceous. In: McCan (Ed.), Geology of Central Europe, vol. 2, 98 pp., London, Geological Society Publishing House

Vonhof, H. B., Jagt, J. W. M., Immenhauser, A., Smit, J., Van den Berg, Y. W., Saher, M., …, Reijmer, J. J. G., 2011. Belemnite-based strontium, carbon and oxygen isotope stratigraphy of the type area of the Maastrichtian Stage. In: Jagt, J. W. M., Jagt-Yazykova, E. A., Schins, W. J. H. (Eds.), A tribute to the late Felder brothers – pioneers in Limburg geology and prehistoric archaeology. Netherlands Journal of Geosciences, 90 (2–3), 259–270, https://doi.org/10.1017/S0016774600001141

Walaszczyk, I., Jagt, J. W. M., Keutgen, N., 2010. The youngest Maastrichtian 'true' inoceramids from the Vijlen Member (Gulpen Formation) in northeast Belgium and the Aachen area (Germany). Netherlands Journal of Geosciences 89 (2), 147–167, https://doi.org/10.1017/S0016774600000755.

Wedepohl, K. H., 1971. Environmental influences on the chemical composition of shales and clays. Physics and Chemistry of the Earth 8, 307–333, https://doi.org/10.1016/0079-1946(71)90020-6.

Wendler, I., 2013. A critical evaluation of carbon isotope stratigraphy and biostratigraphic implications for Late Cretaceous global correlation. Earth-Science Reviews 126, 116–146, https://doi.org/10.1016/j.earscirev.2013.08.003.

Wilmsen, M., Engelke, J., Linnert, C., Mutterlose, J., Niebuhr, B., 2019. A Boreal reference section revisited (Kronsmoor, northern Germany): High-resolution stratigraphic calibration of the Campanian-Maastrichtian boundary interval (Upper Cretaceous). Newsletters on Stratigraphy 52 (2), 155–172, https://doi.org/10.1127/nos/2018/0473.

Woelders, L., Vellekoop, J., Weltje, G. J., De Nooijer, L., Reichart, G.-J., Peterse, F., …, Speijer, R. P., 2018. Robust multi-proxy data integration, using late Cretaceous paleotemperature records as a case study. Earth and Planetary Science Letters 500, 215–224, https://doi.org/10.1016/j.epsl.2018.08.010.

Zijlstra, H. J. P., 1994. Sedimentology of the Late Cretaceous and early Tertiary (tuffaceous) chalk of northwest Europe. Ph.D Thesis, Utrecht University, Utrecht, The Netherlands, 192 p.

Manuscript received: September 28, 2021
Revisions required: October 11, 2021
Revised version received: January 17, 2022
Manuscript accepted: January 18, 2022

The pdf version of this paper includes an electronic supplement

Please save the electronic supplement contained in this pdf-file by clicking the blue frame above. After saving rename the file extension to .zip (for security reasons Adobe does not allow to embed .exe, .zip, .rar etc. files).

Table of contents – Electronic Supplementary Material (ESM)

Supplementary Table 1. $CaCO_3$ content and elemental ratios for Hallembaye and former ENCI quarries.

Supplementary Table 2. Bulk stable carbonate carbon and oxygen isotopic composition of samples from Hallembaye and former ENCI quarries.